POLITECNICO
MILANO 1863

Cooperative Coevolution Approach to Multi-Community Resilience Design

A dissertation for the degree in

Master of Science in Nuclear Engineering

School of Industrial and Information Engineering

Thesis Advisor:

Prof. Enrico Zio

Co-Advisor:

Prof. Giovanni Sansavini

Candidate:

Dario VALCAMONICO

Student Number: 852736

Academic Year: 2017/2018

Acknowledgements

The methodology developed and the results achieved in this thesis are the outcome of the joint effort of the Laboratory of Signal and Risk Analysis LASAR of Politecnico di Milano and the Laboratory of Risk and Reliability Engineering of ETH Zurich. I would like to express my sincere thanks to:

- Prof. Enrico Zio, head of LASAR laboratory at Politecnico di Milano, for giving me the opportunity to work in collaboration with such a high level institution as ETH Zurich.

- Prof. Giovanni Sansavini, head of RRE laboratory at ETH Zurich, for accepting me as a visiting master student in his laboratory. The cooperation, daily discussions and involvement in the life of his laboratory has been extremely helpful not only for the thesis development and the critical evaluation of the results, but also for refining the necessary skills of a high profile researcher.

- The entire RRE group for the hearty welcoming, the professional atmosphere and the deep expertise in the thesis topics, without which this work would not have been possible.

- ETH Zurich institution for easing the bureaucracy, offering a more than pleasant environment and providing the visiting student scholarship.

- The IT Service of the Department of Mechanical and Process Engineering of ETH Zurich for being responsive on the technical difficulties and for providing access to the EULER cluster.

Finally, I would like to thanks my parents Gabriella and Walter Valcamonico, for the invaluable and constant support and encouragement throughout my studies.

Abstract

Despite significant progress in the investigation and deployment of security and safety measures and in the structuring of reliable response protocols in recent years, communities are showing to be still highly vulnerable to natural and man-made hazards. The increasing complexity and interconnectivity of infrastructure systems, which make the critical lifeline of communities has led to a strong emphasis on communities' resilience.

Recovery after disruptions is a key step for building the resilience of communities. This process is influenced by the allocation of resources from different communities and the choice between investments on infrastructure recovery or local emergency solutions. Therefore, the overall community resilience emerges from the coordinated decision-making among the impacted communities and from the trade-off between global and local investments.

This work proposes a methodology for the resilient recovery of interdependent infrastructure systems driven by multi-community decision making, sustained by a cooperative coevolution approach to optimization. The developed simulation model constitutes a practical tool for restoration management. The methodology is tested on benchmark case studies in order to critically evaluate the results and to cope with the computational burden. Moreover, the characteristic of the methodology and its flexibility are discussed.

Key-Words: Community Resilience, Interdependent Infrastructure System Restoration, Multi-Community, Cooperative Coevolution

Sommario

Nonostante i significativi progressi nell'investigazione e applicazione di misure di sicurezza e nella strutturazione di protocolli di risposta affidabili negl'ultimi anni, le *communities* - agglomerati sociali interconnessi - restano altamente vulnerabili a disastri naturali e causati dall'uomo. L'aumentare della complessità e dell'interconnessione dei sistemi di infrastruttura che sostengono le funzionalità delle communities ha imposto una crescente enfasi sulla loro resilienza.

Il recupero post-disastro è un passo fondamentale nello sviluppo di communities resilienti. Tale processo è influenzato dall'allocazione di risorse da communities differenti e dalla scelta di investire nel recupero dei sistemi di infrastruttura o in soluzioni locali di emergenza. Ne segue che la resilienza di una community emerge dal processo decisionale coordinato tra le communities impattate e da una soluzione di trade-off tra investimenti globali e locali.

Questa tesi propone una metodologia per il recupero resiliente di sistemi di infrastruttura interdipendenti guidato dal processo decisionale multi-communitiy, sostenuto da un approccio cooperative coevolution. Il modello di simulazione sviluppato fornisce uno strumento per aiutare la gestione del recupero resiliente post-disastro. La metodologia è testata su casi studio di letteratura con lo scopo di valutare criticamente i risultati e discutere le caratteristiche più importanti.

Parole-chiave: Resilienza, Recupero di Sistemi di Infrastruttura Interdipendenti, Multi-Community, Cooperative Coevolution

Estratto

Capitolo E.1

Introduzione

Nonostante i significativi progressi negl'ultimi anni nell'investigazione e applicazione di misure di sicurezza e nella strutturazione di protocolli di risposta affidabili, le *communities* - agglomerati sociali interconnessi - restano altamente vulnerabili a disastri naturali e causati dall'uomo. L'interruzione della funzionalità di sistemi di infrastruttura critici possono avere conseguenze fisiche, sociali ed economiche catastrofiche [16,17]. La crescente complessità e interconnessione tra tali sistemi e agglomerati urbani complica ulteriormente lo sviluppo di misure protezionistiche.

Grandi sforzi sono stati impiegati nel raggiungere l'obiettivo di resilienza al disastro e studi pioneristici sulla concettualizzazione e quantificazione della resilienza delle communities sono stati sviluppati [5,9,18,24,30,37]. Anche se, in generale, resilienza può essere definita come "l'abilità di rispondere e recuperare da uno scenario di disastro", la sua natura è profondamente "multi-scalare, annidata e sfaccettata" [23].

Una community è una complessa entità che genera e fornisce ai propri abitanti diverse funzionalità e può essere definita come una "rete di interdipendenze socio-economico-organizzative unicamente composta" [30].

Dunque, nonostante le difficoltà nel definire una chiara e standard metrica e fattori consistenti per affrontare il disastro alle communities, un significativo passo in avanti nel caratterizzare e analizzare la resilienza delle communities può concentrarsi sulla funzionalità di quei sistemi di infrastruttura critici che ne sostengono le attività, la sicurezza e il benessere [15].

La capacità di ripristinare la funzionalità post-disastro di tali sistemi dipende dal livello di investimento che communities, decisori e società decidono comunemente di allocare per il recupero. Tuttavia, individualmente ciascuna community potrebbe optare per soluzioni locali a discapito del recupero del sistema e di conseguenza della resilienza delle altre communities. Ne segue che la resilienza multi-community dipende dall'interazione tra il recupero della funzionalità dei sistemi critici di infrastruttura e le decisioni di ciascuna community su misure locali di emergenza.

La seguente tesi propone una metodologia di simulazione per il recupero resiliente di sistemi di infrastruttura interdipendenti che collegano e alimentano più communities. Unitamente alla flessibilità di ciascun modello utilizzato, viene proposto uno strumento simulativo a supporto del processo decisionale di operatori di rete e communities circa le strategie di recupero resiliente multi-community.

Capitolo E.2

Framework per la Resilienza

Resilienza è un concetto diffuso in svariati campi della scienza dalla sociologia alla psicologia, dalla biologia all'ingegneria. Nonostante possa essere definita come "l'abilità di rispondere e recuperare da uno scenario di disastro" numerosi lavori scentifici sono stati dedicati al raggiungere una definizione teorica in grado di coglierne tutti gli aspetti e sfacettature.

Tuttavia, per poter guidare lo sviluppo ingegneristico di un sistema, il concetto di resilienza viene tipicamente quantificato da indici o quantità derivate da caratteristiche misurabili del sistema, le quali vengono combinate sotto ipotesi semplificative. Il risultato è una definizione di resilienza che considera un aspetto specifico ma rilevante all'analisi del sistema in questione.

In questa tesi è stato adottato il framework di resilienza proposto in [31] sia come base concettuale che come strumento di modellizzazione. Tale framework è basato sulla proprietà innata del sistema nel sostenere perturbazioni, denominata *coping capacity*, e sulle azioni di recupero compiute sul sistema prima e dopo l'evento incidentale, in particolare: *retrofit* (miglioramento), l'abilità del sistema di sostenere futuri incidenti, *expansion* (espansione), il complesso di ridondanze e capacità addizionali per sostenere il recupero del sistema, *resource availability* (disponibilità di risorse), la disponibilità di risorse per il recupero del sistema da una condizione incidentale, *response* (risposta), il grado di recupero della funzionalità del sistema.

Le combinazioni di tali azioni e proprietà definiscono le seguenti misure di performance del sistema, illustrate in Fig.E1:

a) *Coping Capacity*: L'abilità innata del sistema di assobire l'impatto del disastro.
b) *Preparedness*: il complesso delle azioni pre-evento prese a prescindere dal verificarsi dell'evento incidentale.

c) *Robustness*: L'abilità del sistema di incrementare la sua resistenza all'evento incidentale.
d) *Flexibility*: opposta alla robustezza, è l'abilità del sistema di adattarsi e rispondere all'evento incidentale.
e) *Recovery*: include le modalità di utilizzo delle risorse per il recupero del sistema post-evento.
f) *Resilience*: l'abilità del sistema di resistere e recuperare dall'evento incidentale.

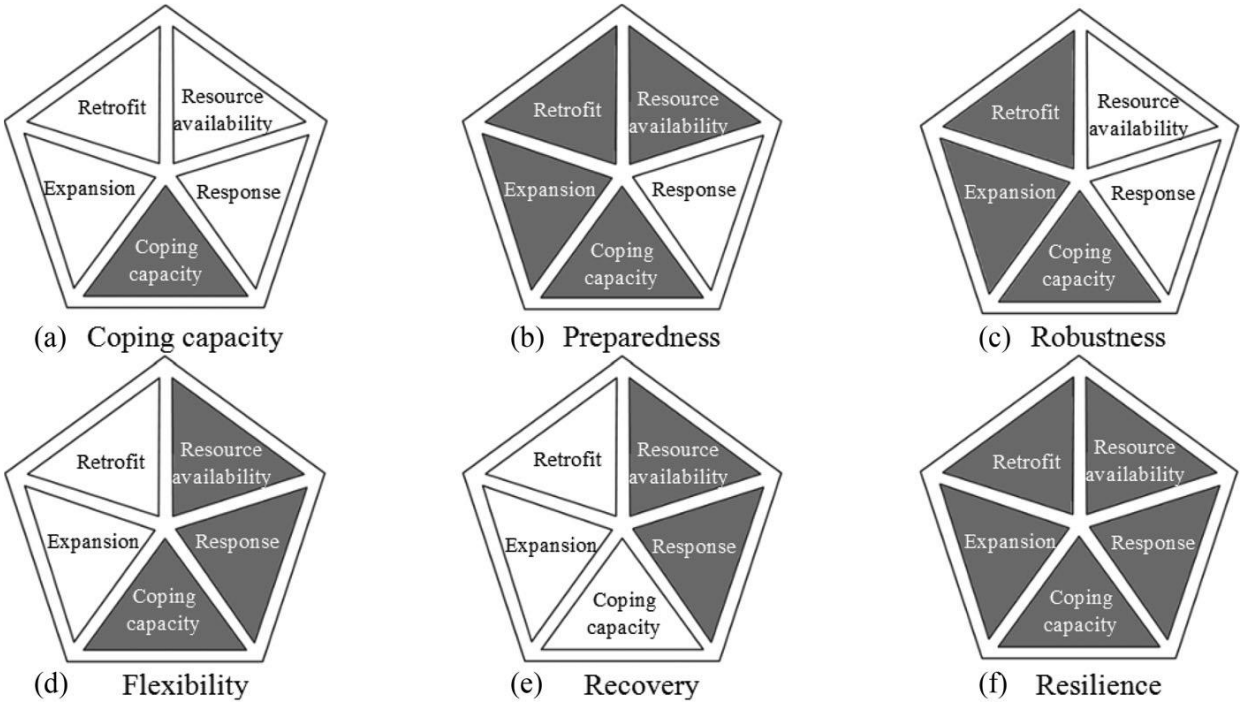

Fig.E1: Le component del framework di protezione del sistema di infrastruttura, rappresentate come combinazione delle abilità innate del sistema e delle azioni pre e post evento incidentale. Immagine presa da [31].

Capitolo E.3

Modelli e Metodi

Approccio Teoria dei Grafi al Sistema di Infrastruttura

I sistemi di infrastruttura interdipendenti considerati in questa tesi sono la rete elettrica e la rete gas. Sono modellati come grafi di N_{nodes}^{k} nodi, indicizzati con i, e N_{edges}^{k} archi, indicizzati con j, dove $k = e$ per la rete elettrica e $k = g$ per la rete gas. I nodi mappano

le stazioni di trasmissione e i consumatori, mentre gli archi rappresentano le linee di connessione attaverso cui le risorse richieste sono trasportate. Per la rete elettrica, i nodi generatori ospitano impianti elettrici che generano potenza elettrica al tempo t, i.e. $P_i^e(t)$, trasmessa ai nodi consumatori per soddisfarne la domanda di carico, i.e. $D_{load,i}^e$. Per la rete gas i nodi generatori sono i terminali di import del gas, i.e. $P_i^g(t)$, per soddisfare la richiesta di gas ai nodi consumatori, i.e. $D_{load,i}^g$. Le domande di carico sono assunte costanti.

L'incidente alla rete causa la perdita di fornimento di risorse ai consumatori. Il disservizio è misurato dalla domanda che non può essere soddifatta al nodo i al tempo t, i.e. $DNS_i^e(t)$ e $DNS_i^g(t)$. Un modello semplificato di trasporto è adottatto, basato su flussi in entrata e in uscita dai nodi, rispettivamente $f_{in,i}^e, f_{in,i}^g$ e $f_{out,i}^e, f_{out,i}^g$, e sull'astrazione dei potenziali elettrici e delle pressioni, ossia ignorando i trasformatori nella rete elettrica ed i compressori nella rete gas. Infine, i bisogni delle communities sono modellizzati come coppie di domande elettriche e gas. L'accoppiamento dei due sistemi di infrastruttura è attraverso le centrali elettriche a gas presenti. Per generalizzazione e semplificazione, i dettagli e la modellizzazione relativi a ciascun componente dei sistemi di infrastruttura sono lasciati all'applicazione specifica.

Conseguenze dell'Incidente sulla Rete

Un semplice modello stocastico di danno è stato adottato. Le linee di trasmissione di ciascun sistema vengono considerate inizialmente alla loro capacità pre-evento. A seguito dell'occorrenza incidentale possono trovarsi in uno stato di totale danno o alcun danno subito. Viene quindi svolta una prova di Bernoulli per ciascun arco delle reti considerate. Se l'arco ha sostenuto il danno la sua capacità è nulla, mentre resta al valore pre-evento in caso contrario. La probabilità di fallimento condizionata all'occorrenza incidentale è assunta 0.2 per gli archi della rete elettrica e 0.3 per gli archi della rete gas, allo scopo di ottenere un grave stato di danno inziale. Il semplice modello stocastico di danno descritto fornisce un punto di partenza conservativo per testare la metodologia sviluppata, considerando la peggior conseguenza di danno in caso di incidente.

Formulazione dei Livelli d'Azione

La resilienza del sistema di infrastruttura si può ottenere implementando misure di recupero e miglioramento sui componenti. Per semplificare senza limitare la decisione su uno specifico set di azioni a priori, viene adottata una descrizione in termini di categorie di azioni. Sulla base di [31] e del framework descritto nel capitolo E.2 vengono introdotte 4 categorie di azioni, sintetizzate in tabella Table E.1. Il livello di ciascuna azione sul j-esimo arco della k-esima rete è caratterizzato da un costo proporzionale al corrispondente massimo, rispettivamente $b_{k,j}^{\alpha}, b_{\alpha}^{max}$ per espansione, $b_{k,j}^{\beta}, b_{\beta}^{max}$ per retrofit, $b_{k,j}^{\gamma}(t), b_{\gamma}^{max}$ per disponibilità di risorse e $b_{k,j}^{\lambda}(t), b_{\lambda}^{max}$ per risposta, come descritto dalle Eqs. (1) - (4).

$$b_{k,j}^{\alpha} = b_{\alpha}^{max}\alpha_j^k \tag{1}$$

$$b_{k,j}^{\beta} = b_{\beta}^{max}\left(1 + \alpha_j^k\right)\beta_j^k \tag{2}$$

$$b_{k,j}^{\gamma}(t) = b_{\gamma}^{max}\gamma_j^k(t) \tag{3}$$

$$b_{k,j}^{\lambda} = \left[b_{\lambda}^{max} - \left(b_{\lambda}^{max} - b_{\lambda}^{min}\right)\gamma_j^k(t)\right]\lambda_j^k(t) \tag{4}$$

La finestra temporale è suddivisa in $t = 1, \dots, N_t$ intervalli considerati come fasi di recupero. Durante ciascuna le azioni di risposta e disponibilità di risorse descritte vengono applicate ad intensità diverse. Nessun tempo implementativo è presente per le azioni di espansione e retrofit in quanto caratteristiche che il sistema possiede prima dell'occorrenza incidentale. Tutte le azioni vengono co-ottimizzate nella metodologia.

Table E1:Definizione e descrizione delle azioni di recupero resiliente e del corrispondente livello.

Azione	Livello d'azione	Significato
Espansione	$\alpha_j^k \in [0,1]$	Percentuale dell'espansione della capacità dell'arco j della rete k. $\alpha_j^k = 1$: capacità dell'arco j della rete k espanso del 100% del suo valore di design.
Retrofit	$\beta_j^k \in [0,1]$	Capacità dell arco j della rete k di assorbire l'impatto del danno in future occorrenze incidentali. $\beta_j^k = 0$: l'arco j della rete k non può sostenere l'impatto del evento incidentale nel futuro. $\beta_j^k = 1$: l'arco j della rete k ha totale capacità di sostenere l'impatto delle future occorrenze incidentali.

Disponibilità di Risorse	$\gamma_j^k(t) \in [0,1]$	Abbondanza di risorse per il recupero e il miglioramento dell'arco j della rete k dopo l'occorrenza incidentale. $\gamma_j^k(t) = 0$: Nessuna disponibilità di risorse per il recupero resiliente dell'arco j della rete k al tempo t. $\gamma_j^k(t) = 1$: Tutte le risorse necessarie per il recupero resiliente dell'arco j della rete k sono presenti e disponibili all'utilizzo al tempo t.
Risposta	$\lambda_j^k(t) \in [0,1]$	Grado di recupero resiliente dell'arco j della rete k nella fase di recupero al tempo t. $\lambda_j^k(t) = 0$: la fase di recupero al tempo t fallisce nel ripristinare la funzionalita dell'arco j della rete k. $\lambda_j^k(t) = 1$: la fase di recupero al tempo t ha complete successo nel ripristinare la funzionalità dell'arco j della rete k.

Ripristino della Capacità dell'Arco

Il recupero della funzionalità della rete di infrastruttura dall'occorrenza incidentale è valutato in termini di recupero resiliente coordinato delle capacità degli archi. In questa sezione viene proposta una definizione matematica flessibile del recupero della capacità dell'arco basata sui livelli di azione presentati nella precedente sezione [31,33,40]. Chiamata $C_{k,j}^{nom}$ la capacità nominale, $C_{k,j}^{dam}$ la capacità post-evento, $C_{k,j}^{\beta}$ la capacità retrofittata e $C_{k,j}^{\alpha\beta}$ la capacità retrofittata e espansa, Eqs. (5) - (6) formalizzano l'implementazione delle azioni di espansione e retrofit:

$$C_{k,j}^{\alpha} = C_{k,j}^{dam} + \beta_j^k\left(C_{k,j}^{nom} - C_{k,j}^{dam}\right) \tag{5}$$

$$C_{k,j}^{\alpha\beta} = C_{k,j}^{\beta}\left(1 + \alpha_j^k\right) \tag{6}$$

Detta $C_{k,j}^{\alpha\beta,max}$ la massima capacità ottenibile solo espandendo e retrofittando l'arco e $C_j^k(t)$ la capacità dell'arco durante la fase di recupero, il processo di recupero dinamico dell'arco è formulato in Eq. (7).

$$C_j^k(t+1) = \begin{cases} \left(C_{k,j}^{nom} + C_{k,j}^{\alpha\beta}\right)\left[1 + \left(\frac{C_{k,j}^{\alpha\beta,max} - C_{k,j}^{dam}}{C_{k,j}^{\alpha\beta,max}}\right)\lambda_j^k(t)\left(1 - e^{-\gamma_j^k(t)}\right)\right] - C_{k,j}^{\alpha\beta} & if\ t = 0 \\ C_j^k(t)\left[1 + \left(\frac{C_{k,j}^{\alpha\beta,max} - C_j^k(t)}{C_{k,j}^{\alpha\beta,max}}\right)\lambda_j^k(t)\left(1 - e^{-\gamma_j^k(t)}\right)\right] & if\ t \geq 1 \end{cases} \tag{7}$$

Un'assunzione tipica nel ripristino dei sistemi complessi è di svolgere prima le operazioni più facili e rapide [40]. Ciò è formalizzato dell'esponenziale negativo in Eq. (7). Nella stessa equazione il rateo che pesa l'esponenziale serve non solo a limitarne la crescita a $C_{k,j}^{\alpha\beta,max}$, ma anche a ridurre di importanza il recupero dell'arco se non ha sostenuto danno nell'occorrenza incidentale. La azioni di recupero resiliente sono implementate in ciascuna fase di recupero con intensità che dipende dalla fase stessa. Ne segue un profilo di capacità esponenziale a tratti come illustrato in Fig. E2.

Dato che le operazioni su ciascun arco avvengono contemporaneamente, il modello proposto implica la presenza di operatori dedicati al recupero di ciascun arco. L'organizzazione delle squadre di recupero non è stata considerata nella metodologia.

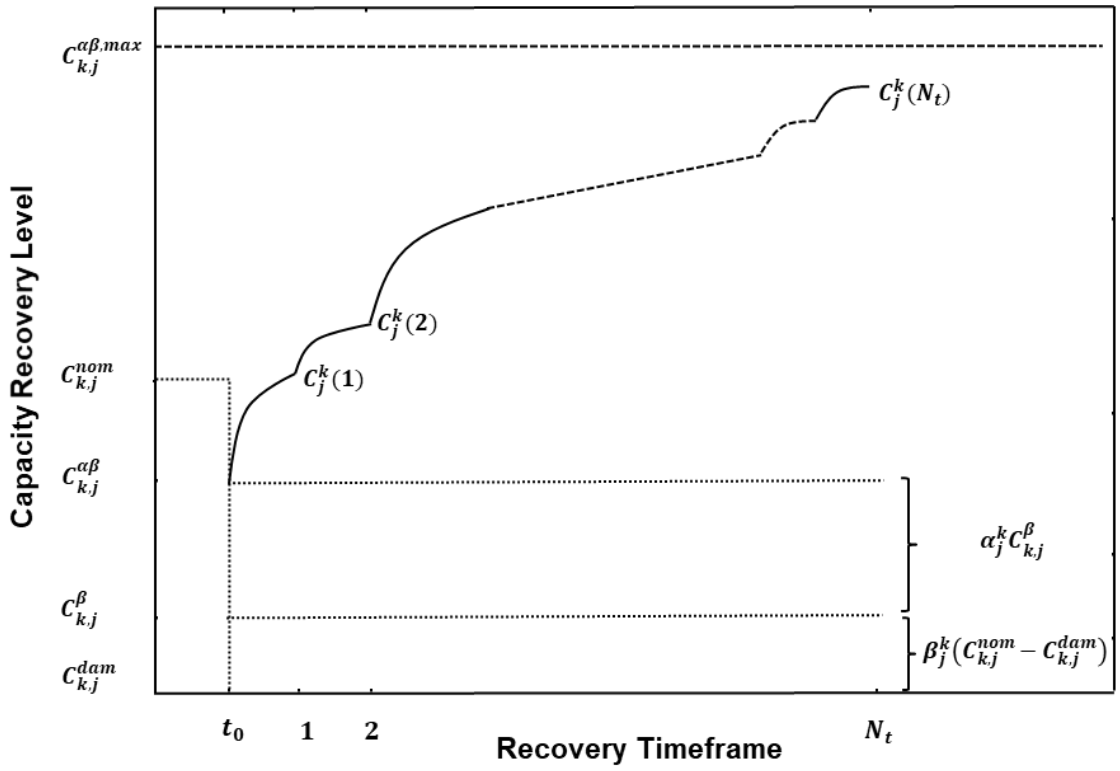

Fig.E2: Illustrazione del processo di recupero della capacità dell'arco dall'occorrenza incidentale a t_0. Il contributo dell'azioni di retrofit e espansione sono rappresentate dalla righe punteggiate. La curva esponenziale a tratti è rappresentata dalla linea continua. L'asintoto della curva esponenziale è rappresentato dalla curva tratteggiata.

Operazione delle Reti e Performance di Recupero

La dinamica dei sistemi di infrastruttura è modellizzata attraverso un approccio a reti di flusso [3]. La metodologia proposta si basa sulla risoluzione di programmi di ottimizzazione multiperiodo vincolati [13,28]. Il programma per quantificare l'operatività delle reti di infrastruttura, minimizza la somma, i.e. $z(t)$, del costo totale di produzione e del costo complessivo dell' insoddisfacimento delle domande di carico al tempo t per ogni k-esima rete, rispettivamente $z_e(t)$ e $z_g(t)$, i.e. Eq. (8), dove $\eta_i^{P_e}$ and $\eta_i^{P_g}$ sono i costi di produzione dell'unità nel nodo i, sotto i vincoli di bilancio di flusso, Eq. (9)-(10), capacità di linea Eq. (11)-(12), capacità generativa, Eq.(13)-(14), e limite della domanda non servita alla domanda di carico Eq.(15)-(16).

$$min \;\; z(t) = z_e(t) + z_g(t) = \sum_{i=1}^{N_{nodes}^e} \left(\eta_i^{P_e} P_i^e(t) + \eta_i^{S_e} DNS_i^e(t)\right) + \sum_{i=1}^{N_{nodes}^g} \left(\eta_i^{P_g} P_i^g(t) + \eta_i^{S_g} DNS_i^g(t)\right) \tag{8}$$

$$\sum_{input\ edges} f_{in,\,i}^e(t) - \sum_{output\ edges} f_{out,\,i}^e(t) + P_i^e(t) - D_{load,i}^e + DNS_i^e(t) = 0\,, \;\; \forall\, i = 1, \dots, N_{nodes}^e \tag{9}$$

$$\sum_{input\ edges} f_{in,\,i}^g(t) - \sum_{output\ edges} f_{out,\,i}^g(t) + P_i^g(t) - D_{load,i}^g + DNS_i^g(t) = 0, \;\; \forall\, i = 1, \dots, N_{nodes}^g \tag{10}$$

$$0 \le \left|f_j^e(t)\right| \le C_j^e(t) = f(\alpha_j^e, \beta_j^e, \gamma_j^e(1), \gamma_j^e(1), \dots, \gamma_j^e(N_t), \lambda_j^e(N_t)) \qquad \forall\, j = 1, \dots, N_{edges}^e \tag{11}$$

$$0 \le \left|f_j^g(t)\right| \le C_j^g(t) = f\left(\alpha_j^g, \beta_j^g, \gamma_j^g(1), \lambda_j^g(1), \dots, \gamma_j^g(N_t), \lambda_j^g(N_t)\right) \quad \forall\, j = 1, \dots, N_{edges}^g \tag{12}$$

$$P_{min,i}^e \le P_i^e(t) \le P_{max,i}^e \quad \forall\, i = 1, \dots, N_{nodes}^e \tag{13}$$

$$P_{min,i}^g \le P_i^g(t) \le P_{max,i}^g \quad \forall\, i = 1, \dots, N_{nodes}^e \tag{14}$$

$$0 \le DNS_i^e(t) \le D_{load,i}^e \quad \forall\, i = 1, \dots, N_{nodes}^e \tag{15}$$

$$0 \le DNS_i^g(t) \le D_{load,i}^g \quad \forall\, i = 1, \dots, N_{nodes}^e \tag{16}$$

La performance della rete di flusso è quantificata dal massimo flusso/servizio aggregato che può essere fornito alle communities, i.e. Eq.(17) dove $D_l^k(t)$ è la domanda di carico della rete di infrastruttura k che può essere fornita alla comunità l al tempo t. La massima domanda allocabile alla community pertanto rappresenta una misura della capacità del sistema di infrastruttura di trasmettere il suo servizio ed è usata come misura di performance del recupero della rete [27]. Eqs. (17) - (24) formalizzano il rispettivo programma di ottimizzazione.

$$max \sum_{l=1}^{N_{communities}} D_l^k\,(t) \qquad \forall k\ commodity \tag{17}$$

$$\sum_{input\ edges} f_{in,\,i}^{e}(t) - \sum_{output\ edges} f_{out,\,i}^{e}(t) + P_i^e(t) - D_i^e(t) = 0\ ,\ \ \forall\, i = 1, \dots, N_{nodes}^{e} \tag{18}$$

$$\sum_{input\ edges} f_{in,\,i}^{g}(t) - \sum_{output\ edges} f_{out,\,i}^{g}(t) + P_i^g(t) - D_i^g(t) = 0,\ \ \forall\, i = 1, \dots, N_{nodes}^{g} \tag{19}$$

$$0 \le \left|f_j^e(t)\right| \le C_j^e(t) = f\left(\alpha_j^e, \beta_j^e, \gamma_j^e(1), \gamma_j^e(1), \dots, \gamma_j^e(N_t), \lambda_j^e(N_t)\right) \qquad \forall\, j = 1, \dots, N_{edges}^{e} \tag{20}$$

$$0 \le \left|f_j^g(t)\right| \le C_j^g(t) = f\left(\alpha_j^g, \beta_j^g, \gamma_j^g(1), \lambda_j^g(1), \dots, \gamma_j^g(N_t), \lambda_j^g(N_t)\right) \quad \forall\, j = 1, \dots, N_{edges}^{g} \tag{21}$$

$$P_{min,i}^{e} \le P_i^e(t) \le P_{max,i}^{e} \quad \forall\, i = 1, \dots, N_{nodes}^{e} \tag{22}$$

$$P_{min,i}^{g} \le P_i^g(t) \le P_{max,i}^{g} \quad \forall\, i = 1, \dots, N_{nodes}^{e} \tag{23}$$

$$D_l^k \ge 0 \quad \forall l\ community, \forall k\ commodity \tag{24}$$

Cooperative Coevolution e Processo Decisionale della Community

Un modello multi-agente è adottato per il processo decisionale delle communities. L'obiettivo di ciascun agente, è la massimizzazione della resilienza della community corrispondente, misurata dalla massima domanda allocabile a tale community l, i.e. Eq. (25).

$$max\ D_l^k\,(t) \qquad \forall k\ commodity \tag{25}$$

A causa della tensione tra l'allocamento di budget per il ripristino della rete di infrastruttura condivisa e per una soluzione di emergenza locale, le decisioni delle communities potrebbero essere contrastanti. Per risolvere tale conflitto viene introdotto un agente astratto, chiamato operatore del sistema di trasmissione (TSO), il cui obiettivo è la massimizzazione del recupero resiliente della rete per cercare un accordo tra tutte le communities, ossia l'Eq. (17).

Allo scopo di trovare una soluzione di compromesso multi-obiettivo, è stato introdotto un modello metaeuristico basato sull'algoritmo Cooperative Coevolution (CC) [21,26]. L'obiettivo di ogni agente può, infatti, essere considerato come una possibile euristica per l'ottimizzazione della soluzione di recupero, ossia il set di livelli di azione di recupero da implementare su ciascun arco delle reti di infrastruttura. Per superare le difficoltà

poste dall'alto livello di non-linearità dei programmi di ottimizzazione descritti sopra e del processo di recupero della capacità, un metodo di Differential Evolution (DE) è utilizzato come strumento di ottimizzazione della soluzione di recupero [35]. L'algoritmo risolutivo consiste nell'ottimizzazione, iterativa e non-greedy, del set di livelli di azione da compiere sulla rete, indipendentemente per ciascuna euristica. Tale modulo è indicato come *DE-step*. Tali soluzioni vengono poi confrontate fra loro e valutate dagli agenti communities e TSO, nel modulo indicato come *Conversation step*, e la miglior soluzione di compromesso, sotto il vincolo di performance di recupero e soddisfacimento delle domande di carico, viene ottenuta. L'interazione dei diversi moduli della metodologia è illustrata in Fig.E3.

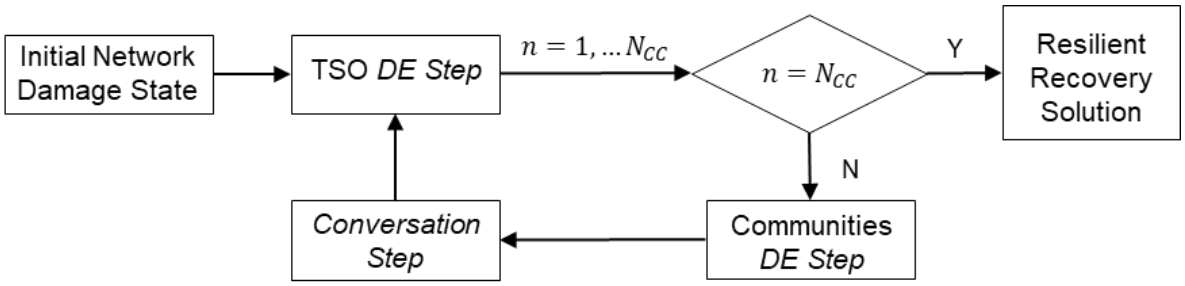

Fig.E3: Interazione dei moduli della metodologia di recupero. Le soluzioni ottimizzate secondo l'euristica dell'agente TSO e degli agenti communities (DE Step), vengono confrontate (Conversation Step) e ri-ottimizzate iterativamente, verso la miglior soluzione di compromesso.

Capitolo E.4

Applicazione e Risultati

Caso Studio

La metodologia è testata su una piccola rete benchmark [38] rappresentata in Fig. E4. Accoppiando le domande di carico elettrici e gas 3 communities sono individuate: ($D^e_{load,1}$, $D^g_{load,1}$), ($D^e_{load,2}$, $D^g_{load,2}$) e ($D^e_{load,3}$, $D^g_{load,3}$). Per motivi di rappresentazione, l'orizzonte di recupero è fissato ad un mese e $N_t = 4$ step temporali sono considerati. La metodologia è implementata e risolta con il software MATLAB e i programmi di

ottimizzazione sono risolti con GUROBI [14] via YALMIP [20]. I risultati sono stati ottenuti da simulazioni risolte attraverso il cluter EULER presso ETH Zurich. Il tempo totale di computazione è di 11576 secondi.

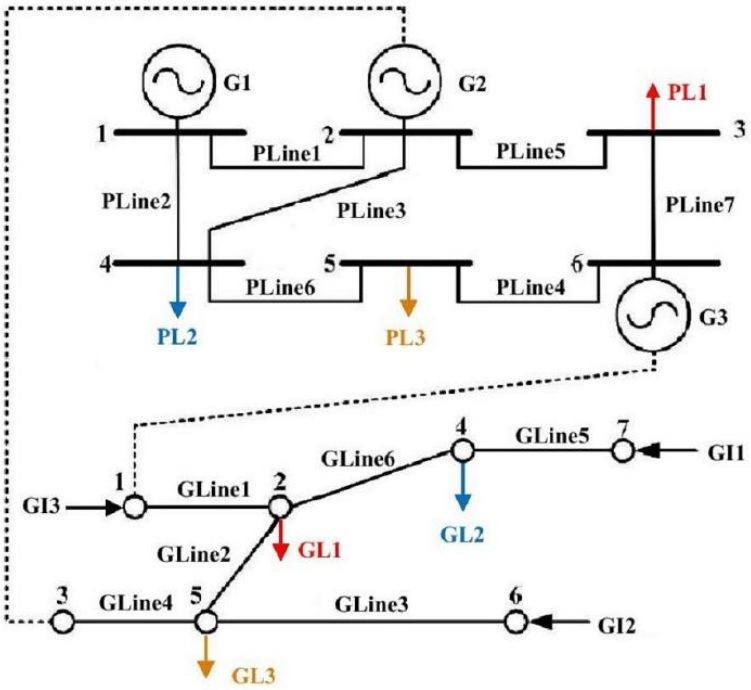

Fig.E4: Rappresentazione della rete caso studio. G: generatore elettrico, GI: terminale import gas, PLine: arco rete elettrica, GLine: arco rete gas, PL: domanda di carico elettrica, GL: domanda di carico gas. 3 communities: (PL1,GL1) in rosso, (PL2,GL2) in blu, (PL3,GL3) in giallo.

Configurazione di Danno della Rete

I risultati della metodologia di recupero sono rappresentati a partire dalla configurazione stocastica di danno rappresentata in Fig. E5. La disconnessione dei generatori elettrici G2 e G3 provoca un'alta DNS_2^e (PL2) e DNS_3^e (PL3), e similmente nella rete gas solo $D_{load,1}^g$ (GL1) è soddisfatta. Il recupero della rete deve dunque tendere al ripristino degli archi PLine1, PLine2, GLine3 e GLine5 per garantire il fornimento di risorse dai generatori.

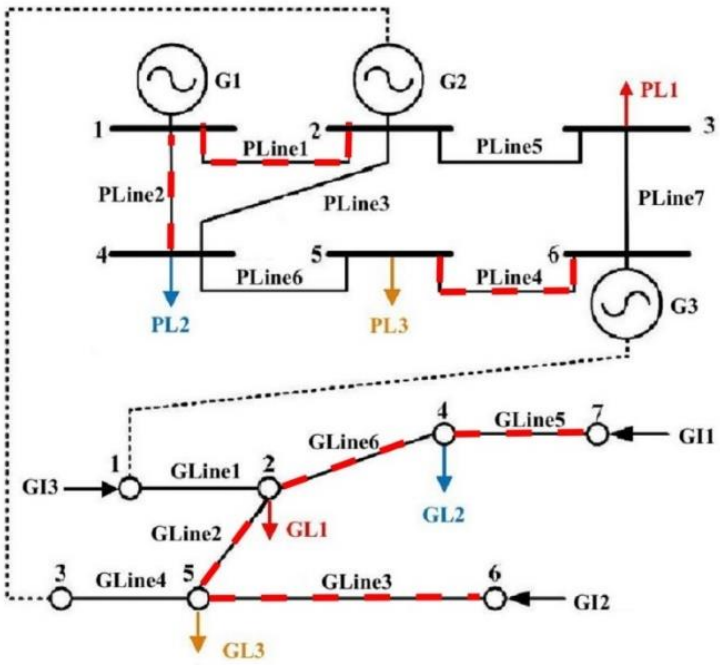

Fig.E5: Stato di danno iniziale. In rosso tratteggiato gli archi distrutti.

Recupero della Rete

Il processo di recupero della rete è illustrato in Fig.E6. La metodologia si dimostra in grado sia di ripristinare la funzionalità degli archi danneggiati che di migliorare gli archi sani. Ne segue un processo di recupero della rete in grado di assorbire l'impatto dell'occorrenza incidentale, in quanto il danno ad un arco può essere aggirato rafforzando gli archi circostanti. Ciò può essere notato ad esempio dal rafforzamento dell'arco sano PLine3 rispetto al recupero dell'arco distrutto PLine2. Ne segue che la metodologia si dimostra in grado di trovare configurazioni alternative di rete per soddisfare le domande di carico.

Come atteso, l'algoritmo ripristina le connessioni tra le communities e i generatori nella finestra temporale di recupero considerata. Inoltre vi è una tendenza ad irrobustire gli archi con la capacità minore, come conseguenza diretta del guidare la metodologia di recupero con la massima domanda allocabile alla community, purchè sia garantito il soddisfacimento delle domande di carico. Ciò è osservabile ad esempio nel grado di recupero di GLine4 rispetto a GLine3 essendo la capacità nominale di GLine3 molto più grande che di GLine4.

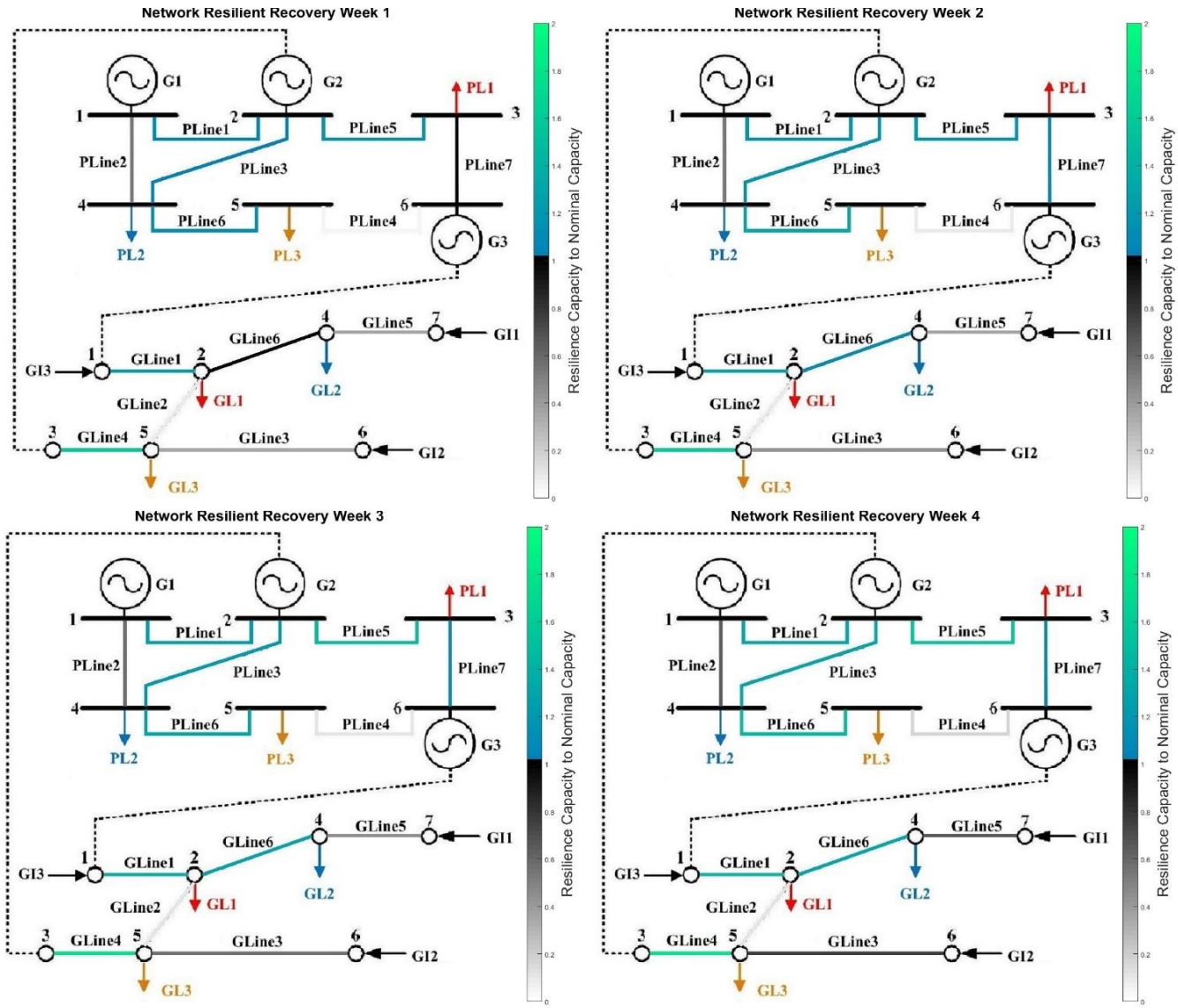

Fig.E6: Recupero Resiliente della rete. Il rapporto tra la capacità recuperate e la capacità nominale degli archi è rappresentata sullo schema della rete in ogni step temporale.

Le curve di massima domanda allocabile e di domanda non servita alle communities sono rappresentate rispettivamente in Fig. E7 e Fig. E8. Dato che la metodologia guida il recupero attraverso la massima domanda allocabile totale alle communities e cerca di trovare una soluzione di compromesso, le singole massime domande allocabili a ciascuna community possono diminuire in favore di altre se vi è un guadagno di performance generale. Allo stesso tempo, la funzione obiettivo della metodologia è tale per cui una soluzione che non soddisfa le domande di carico viene fortemente penalizzata. Dalle curve in Figs.E7-E8 è verificabile come la soluzione di recupero soddisfi tutte le domande di carico. Da quest'ultime, è inoltre verificabile come le curve di recupero proposte da agenti community e TSO siano sovrapposte. L'alto livello di coordinazione è da attribuire principalmente alle ridotte dimensioni della rete, tali per cui le soluzioni ottimali di recupero della rete per ciascuna community sono simili fra loro.

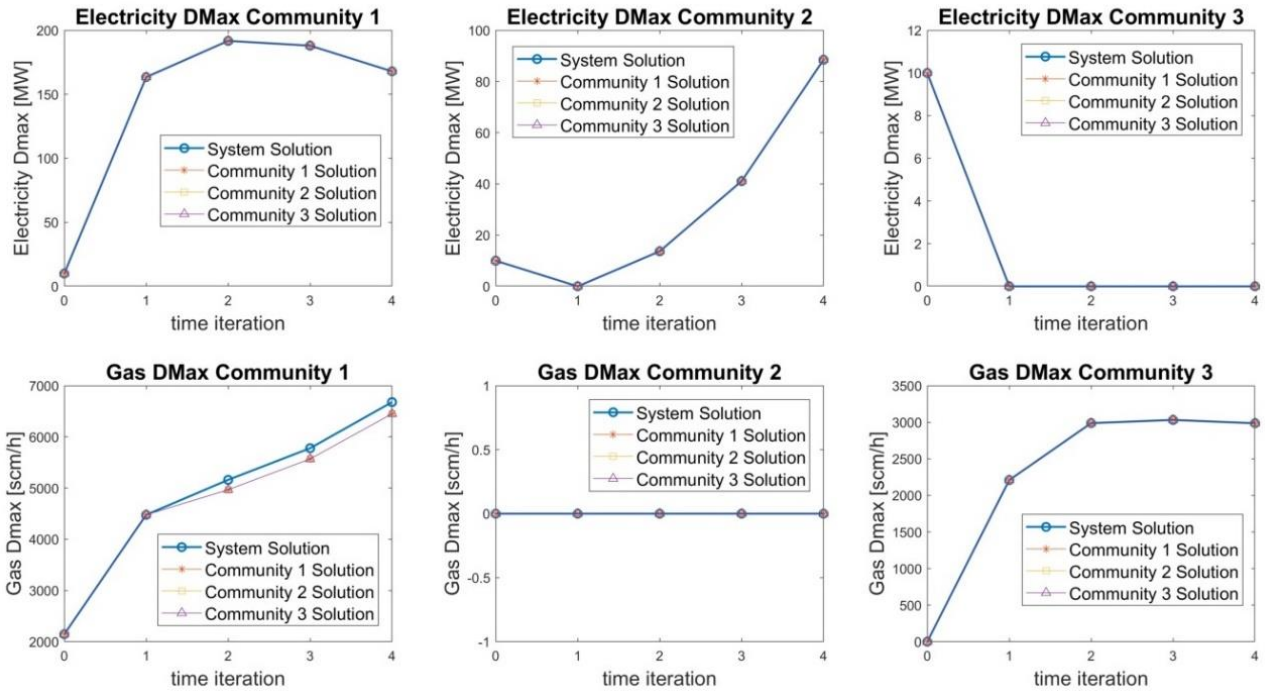

Fig.E7: Massima domanda elettrica e gas allocabile alle communities. I risultati di ciascun agente decisionale illustrati sono riferiti all'ultima iterazione della metodologia.

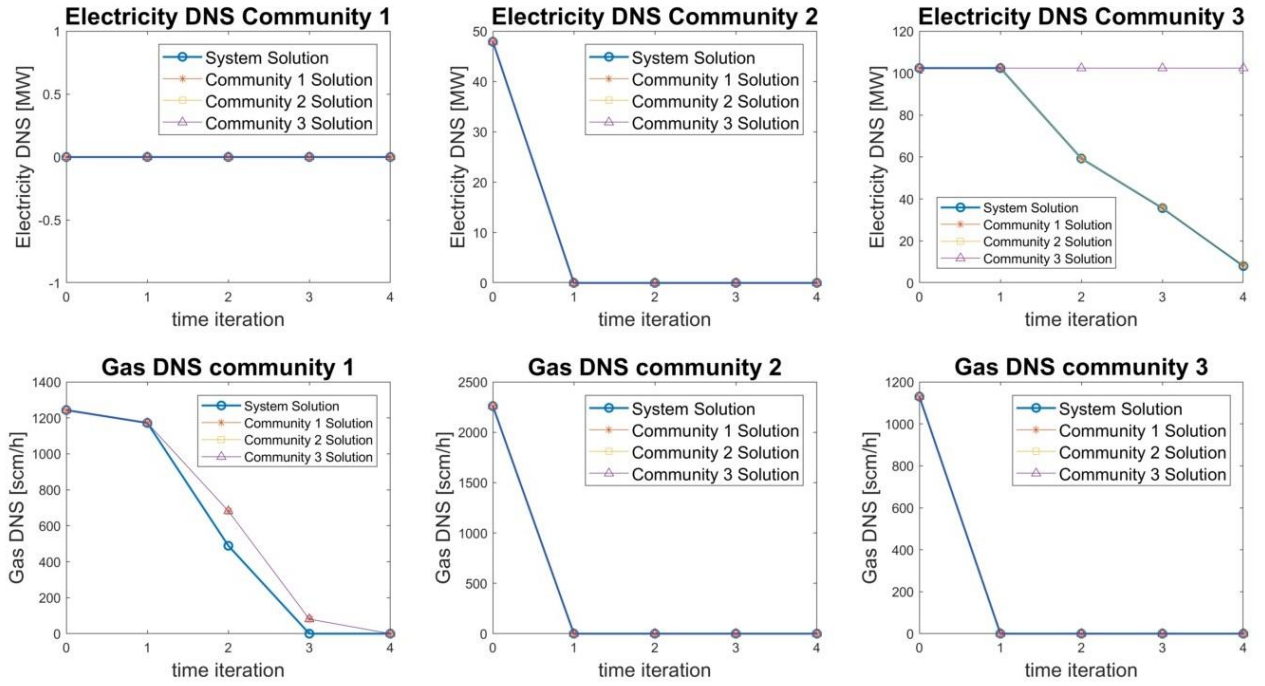

Fig.E8: Domande non servite elettrica e gas. I risultati illustrate di ciascun agente decisionale sono riferiti all'ultima iterazione della metodologia.

Configurazioni di Recupero della Rete

A partire dallo stato di danno iniziale in Fig. E5, la metodologia di recupero è testate $N_k = 50$ volte indipendentemente. Le 2 migliori configurazioni di recupero, ossia quelle con performance di recupero più alte, sono rappresentate in Fig. E9. La differenza più evidente è nel recupero della rete gas. Mentre nella configurazione a sinistra in Fig. E9 gli archi adiacenti alle community vengono favoriti, la soluzione rappresentata a destra propone una configurazione meno rinforzata ma più connessa. Ciò testimonia come la metodologia sia in grado di esplorare configurazioni di recupero performanti diverse ma competitive. La flessibilità dei modelli introdotti consente l'introduzione di vincoli specifici per guidare le soluzioni di recupero nell'applicazione specifica.

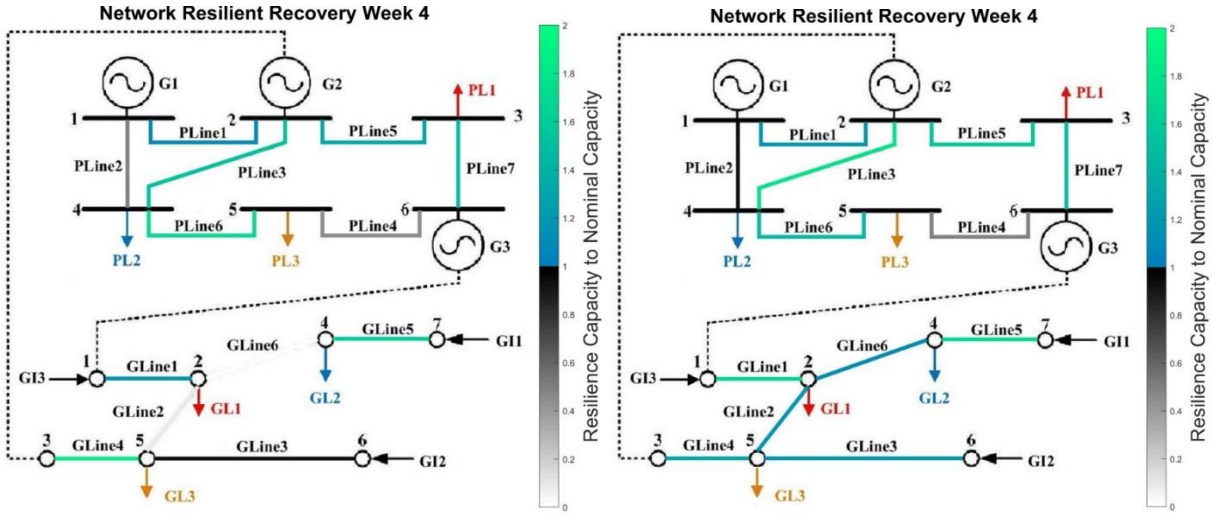

Fig.E9: 2 configurazioni di recupero della rete più performanti da 50 run indipendenti della metodologia dallo stesso stato di danno iniziale.

Scalabilità della Metodologia di Recupero

La metodologia è testata anche sulla rete benchmark [38] in Fig. E10, composta da una rete elettrica 39 nodi e una rete gas 20 nodi, rappresentativa della rete gas Belga. 9 communities sono individuate accoppiando le domande di carico elettrico e gas, mentre le restanti 9 domande di carico rappresentano communities basate solo su load elettrico. I modelli utilizzati e il livello di dettaglio sono identici al precedente caso studio, e pertanto la metodologia di recupero è applicata per studiarne la scalabilità ad un caso studio di dimensione maggiore.

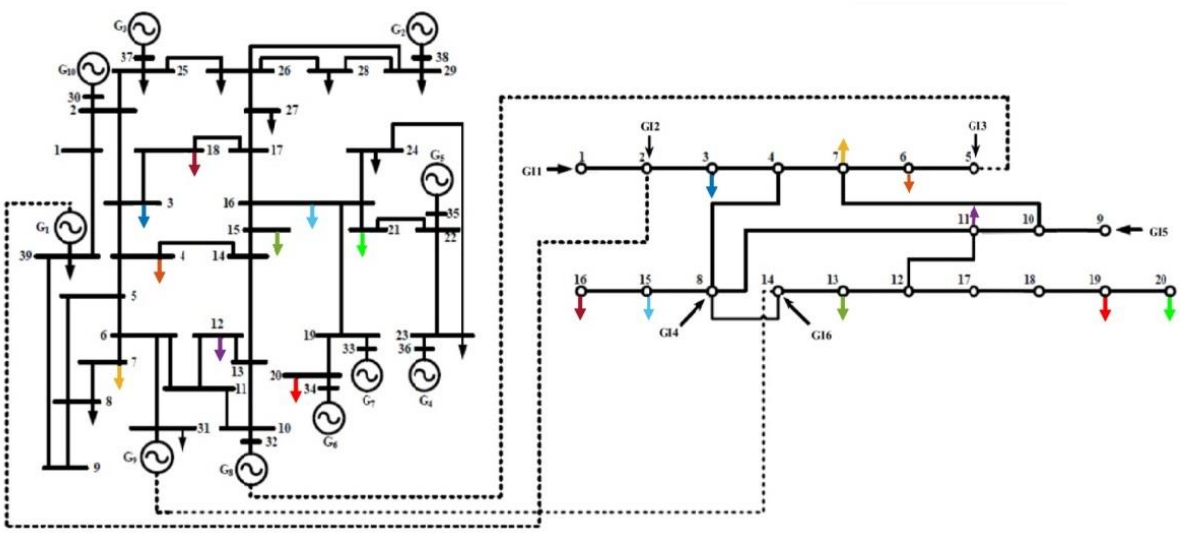

Fig.E10: Caso studio 39-bus rete elettrica e 20-bus rete gas. 9 communities sono individuate accoppiando load elettrico e gas.

Lo stato di danno iniziale in Fig. E11 comporta la totale o parziale disconnessione dei generatori elettrici G1, G7, G10, G8, G9 e G5 e la rottura di archi di connessione importanti come dal nodo 13 al nodo 14. Similmente nella rete gas, i terminali import GI1, GI2 e GI3 sono disconnessi.

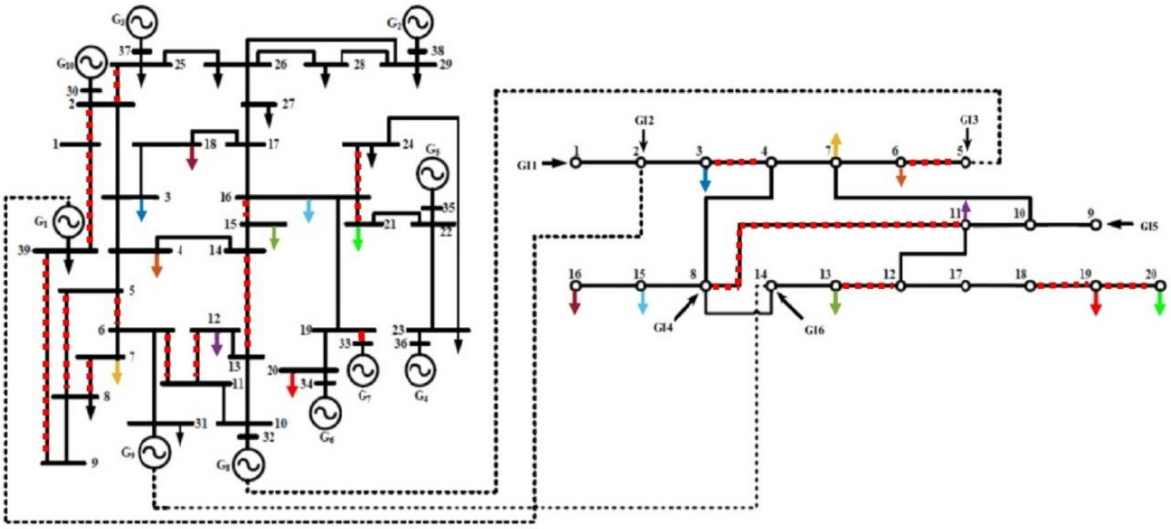

Fig.E11: Condizione di danno inziale del caso studio 39-bus rete elettrica e 20-bus rete gas.

Il recupero in Fig.E12 mostra risultati simili al caso studio precedente. Tutti i generatori elettrici vengono riconnessi alla rete ad esclusione di G1 a causa della domanda elettrica al nodo 39 immediatamente adiacente. Similmente nella rete gas gli archi più importanti vegono rinforzati a sfavore di archi ridondanti, ad esempio l'arco tra il nodo 8 e il nodo 11.

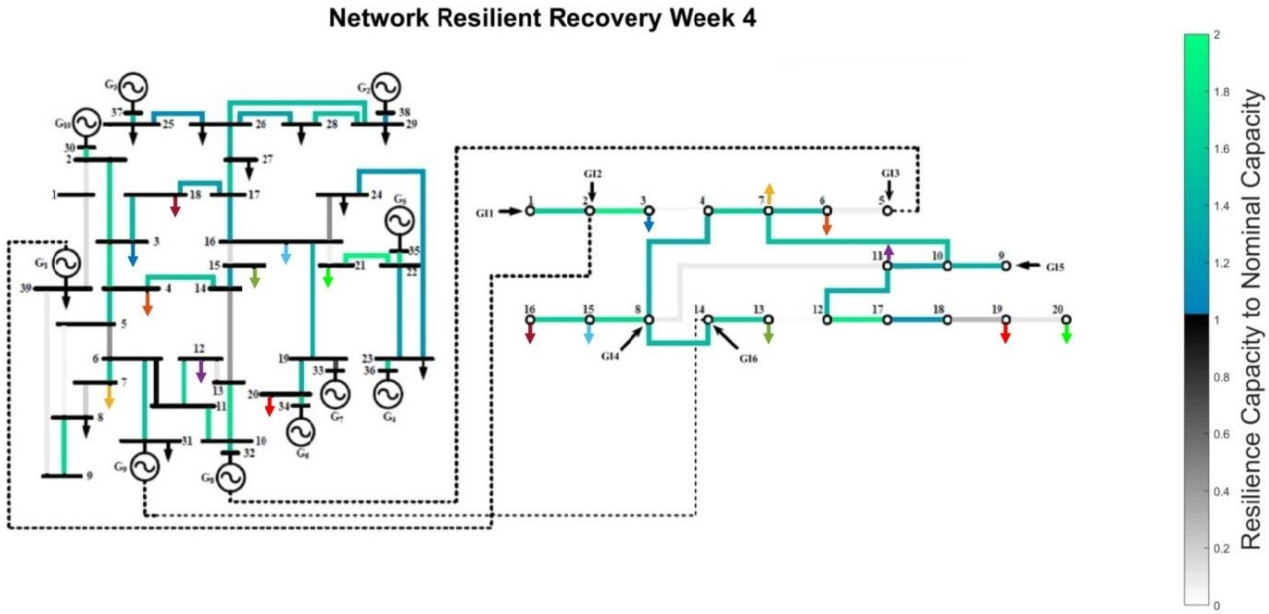

Fig.E12: Configurazione di recupero del caso studio 39-bus rete elettrica e 20-bus rete gas.

Conclusione

Questa tesi presenta una metodologia di recupero resiliente da un'occorrenza incidentale di sistemi di infrastruttura interdipendenti, guidata da un processo decisionale multi-community. Uno schema di cooperative coevolution è utilizzato per coordinare ciascun agente decisionale, ottenere una soluzione trade-off e ottimizzare le azioni da compiere sul sistema. La metodologia presenta un alto grado di flessibilità, in quanto ciascun modello è estendibile e integrabile a specifici casi studio o analisi. I concetti chiave di resilienza sono trattati nell'ambito della teoria delle reti e in una generale definizione di categorie di azioni da compiere, allo scopo di non vincolare la soluzione di recupero ad una particolare strategia a priori.

L'applicazione a due casi studio di letteratura ha condotto ai seguenti risultati principali:

- La metodologia propone una soluzione di compromesso coordinata tra gli agenti decisionali in grado di ripristinare la funzionalità della rete di infrastruttura e soddisfare le domande di carico delle communità.
- I risultati della soluzione di recupero della rete dipendono dalla dimensione e configurazione di quest'ultima, e sono coerenti con il dataset e le assunzioni dei modelli impiegati.

La metodologia sviluppata è un approccio preliminare al problema di resilienza multi-community e pertanto non ottimale per sistemi reali e su larga scala. Nonostante ciò, la

coerenza dei risultati, la flessibilità ed estendibilità di ciascun modulo della metodologia, e la capacità dello schema di cooperative coevolution di racchiudere in un'unica struttura metaeuristica l'ottimizzazione multi-obiettivo, giustificano l'analisi condotta in questa tesi.

Contents

List of Figures

Chapter 1

Introduction

Social-welfare and security are regarded as the most important aspects to preserve and improve in today's societies. The interruption of critical infrastructure systems functionality, that provide services and goods to end users, can have catastrophic economic and social consequences [16,17]. Natural and man-made hazards are responsible each year for massive damage to communities, due to these lasts increasing vulnerability and exposure together with the increasing hazard events frequencies [30,34]. For example, in the US a $57 billion of annual average total costs are estimated, accounting for fatalities, emergency services to deploy, damage to properties and disruption of economic activities [8]. The growing complexity and interconnectivity between systems and urban agglomerates further complicates the development of protection measures.

Much effort is being devoted to achieve disaster-resilient communities and pioneering work has been developed in the conceptualization and quantification of community resilience [5,9,18,24,30,37]. While in general resilience can be regarded as the "ability to respond and recover from disasters" [9], its nature is deeply "multi-scalar, nested and multifaceted" [23]. A community is a deeply complex entity which generates and provides various functionalities to its inhabitants and is characterized by a "uniquely arranged network of socio-economic-organizational interdependencies", and typically in a multi-community setting [30]. While extremely challenging to define, a sensible effort to analyze and characterize community resilience after a disruptive event can focus on the functionality of those critical infrastructure, which support the community security and well-being [15].

Yet, "while numerous research efforts have assessed various dimensions of community resilience, challenges remain in the development of consistent factors or standard metrics that can be used to evaluate the disaster resilience of communities" [9].

Generally, the capability of infrastructure systems to regain functionality and providing services after a disruption is related to the level of investments that communities, decision makers and society jointly allocate to their recovery and restoration. On the other hand, individual communities may ensure a sufficient level of service provision via investments in local buffers, generation and stockpile; this strengthen the resilience of the local community

but can possibly divert resources from infrastructure restoration, and, ultimately, impair the resilience of other communities. Inevitably, then, community resilience results from the interplay between the functionality of critical infrastructures and the local community resourcefulness. This situation calls for the need of finding an optimum trade-off between multi-community investments by society as a whole for restoring critical infrastructure and single community investments on local resources for the times of service disruption.

Safety and security protocols and protection measures are usually installed in infrastructure systems, to aid the control during normal operations and automatize the recovery in accidental ones. Nevertheless, experience shows that communities are deeply involved in the response to disasters. Therefore, an effort is necessary to include community decision making in the infrastructure system restoration process where several players are involved in the decision and multiple objectives have to be considered at once. Treating whole communities as interacting agents can be a possible solution to model both the community internal organizational dynamics and the cooperation between communities and system decision makers [8]. For example in [29] a multi-agent Bayesian model is adopted for customers' decision making, to feedback the disaster risk management, and in [38] a place-based agent model is exploited to analyze the influence of the interaction between system protection measures and individual behavior to community flood risk

This thesis contributes to the aforementioned effort by investigating how the level of coordination among communities supported by shared critical infrastructures for allocating restoration resources affects their overall resilience. Modelling for multi-agent decision making on infrastructure systems recovery is addressed within a cooperative coevolution metaheuristics scheme, which allows a flexible structure of the multi-objective agent-based optimization for including the infrastructure systems dynamics and its restoration process, avoiding the computational difficulties of traditional optimization techniques.

We model community decision-making and its integration with the infrastructure systems performance as a multi-community recovery simulation, which determines the resilience of the entire system of communities. From the hazard occurrence, the damage of the infrastructure systems is initialized. The network recovery simulation combines the implementation of resilience actions, the restoration actions to perform on the network components, and multi-community decision making, and provides a flexible simulation tool to the transmission system operators and communities about strategies for designing resilient infrastructure systems.

The methodology developed in this thesis focuses on the restoration of interdependent energy infrastructure systems after a hazard occurrence. For illustration purposes, the interactions between the electric and gas supply networks are considered, being among the most studied commodity networks in literature [2,3]. Nonetheless, the developed methodology can be extended to include other critical infrastructure systems such as water distribution, communication systems and road networks. While their interdependencies are fundamental to be addressed, as a contingency in one network could propagate in the connected one and cascading failure issues arise [19], in this work simple network models are adopted and the infrastructure systems interaction is not modeled in depth.

Overall, the research objectives can be summarized as follows:

- Develop simple and effective models for infrastructure systems, communities and resilience.
- Investigate the interplay of each model to provide a simulation tool for the resilient restoration of the system from a disaster scenario.
- Set up a flexible solution methodology able to embed different objectives and solve the problem from a multi-community perspective.
- Critically evaluate results and the capability of the methodology to provide a reliable answer.

The remainder of the thesis is organized as follows:

- In Chapter 2 the resilience framework adopted throughout the thesis is presented.
- In Chapter 3 all the models used are detailed, together with the simplifying and modeling assumptions; the solution methodology and the interplay of each module are also exposed.
- In Chapter 4 the case study application and the main results and analysis performed are presented;
- in Chapter 5 the conclusions and further lines of investigation are drawn.

Chapter 2

Resilience Framework

Resilience is a widespread concept in many disciplines ranging from sociology and psychology to economics and engineering. An accepted definition is “the ability to withstand and recover from a hazard occurrence”, and applied to the field of disaster mitigation it can be thought to include the “measures that seek to prevent hazard-related damage and losses and post-event strategies designed to cope with and minimize disaster impacts” [5]. But, the nature of resilience is “multi-scalar, nested and multifaceted” [23], and rather than being an inherent property of the system, it is an evolving and cohesive feature that characterize the system from the design phase to the end of life, that it acquires through time, expresses in different ways and can be categorized and studied under different labels.

Nevertheless, in order to provide engineering answers and guide the system development, the concept of resilience is usually reduced down to a quantity or index, computed or optimized from other measurable characteristic or properties, which are combined in a certain way under simplifying assumptions. The result is usually a parameter that highlights specific resilience aspects of the system that are of primary importance to be addressed.

Several performance measures have been used in literature to quantify the ability of a system to reduce risks of failure and increase the system ability to rebound from disasters. Throughout this thesis the framework proposed in [31] is adopted both as a conceptual basis and modeling tool. The “infrastructure protection framework” develops from the innate properties of the system to sustain perturbations, namely *coping capacity*, and pre-event and post-event actions and prevention measures that can be implemented to help the system recover its functionality. These last include: *retrofit*, the ability of the system to sustain future hazard occurrences, *expansion*, in terms of redundancies and additional capacity to aid system in shock and recovered scenarios, *resource availability*, which intensity is directly correlated to the restorative performance, and *response*, the degree of recovery of the system functionality. The critical performance measures of the system are defined as combination of the above mentioned actions and schematized in Fig.1:

a) Coping Capacity: the innate ability of the system to absorb the impact of the hazard.

b) *Preparedness*: the complex of pre-event actions that are taken regardless of the hazard event occurrence.

c) *Robustness*: the ability of the system to enhance its resistance under disruption, and different from coping capacity as it considers also the implemented expansion and retrofit level.

d) *Flexibility*: opposite to robustness, it is the ability of the system to adapt and respond to the hazard, regardless of the preventive action implemented and therefore dealing only with post-event action and innate ability.

e) *Recovery*: includes how the resources and the post-event action are capable of restoring the system functionalities, regardless of the innate and pre-event actions.

f) *Resilience*: the overall ability of the system to withstand and recover from the hazard occurrence.

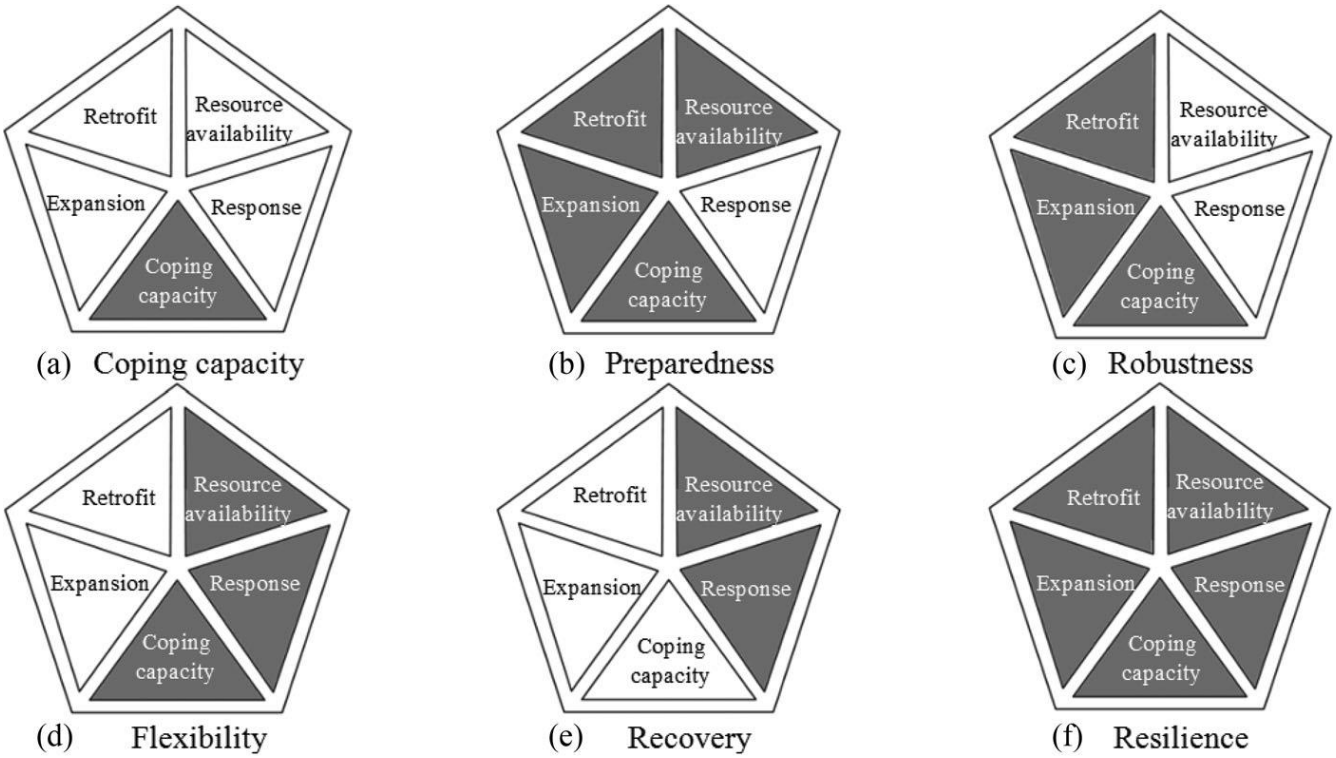

Fig. 1: Infrastructure protection framework components, visually represented as combination of system innate abilities, pre-event and post-event actions. Image from reference [31].

The resilience framework just introduced, together with the network-based approach detailed in the next section, set the basis for a flexible methodology that can be generalized and adopted for different kinds of systems. More importantly, it is developed consistently from key resilience concepts, separated and combined already at a conceptual level.

Chapter 3

Models and Methods

In this chapter the models used in the thesis, the methods applied and the interplay of each part are presented together with the main simplifying assumption. First, in section 3.1 the network model of the infrastructure systems is detailed. Then, in Section 3.2 a stochastic hazard model for system components is described. The resilience actions definition and the related mapping into action levels is presented in Section 3.3 followed by the recovery process of networks' edges in Section 3.4. Section 3.5 introduces the network commodity flow operation and network recovery performance optimization programs. Finally, in Section 3.6 the solution methodology is presented by illustrating the interplay of two modules: the optimization method *DE-step*, based on the evolutionary algorithm Differential Evolution and embedded with single community decision making, and the agent based multi-objective model called *Conversation Step*. Together, they define the *Cooperative Coevolution* metaheuristics, which, starting from a hazard occurrence, co-optimizes and coordinates multi-community recovery solutions, towards a trade-off network restoration strategy for resilience.

3.1) Network Approach to Infrastructure System

Graph theory is often used for infrastructure system modeling [10]. Electric power grids and gas networks are modeled, as graphs of N_{nodes}^{k} nodes, indexed with i,and N_{edges}^{k} edges, indexed with j, where $k = e$ for the electric grid and $k = g$ for the gas network. Nodes map commodity specific transmission stations and consumer wells, whereas edges map connection lines where commodities flow.

For the power grid, generator nodes host power plants generating electrical power at time t, i.e. $P_i^e(t)$, which is transmitted along power lines and distributed to consumer nodes, i.e. $D_{load,i}^{e}$.For gas network, generator nodes are the gas import terminals, i.e. $P_i^g(t)$, providing

the required gas demand to consumers, i.e. $D^{g}_{load,i}$, along dedicated pipelines. The load demands are assumed constant throughout the model.

The disruption of the network causes the loss of commodities supply to communities and eventually the disconnection of generators from the network. The disservice to consumers is measured by the demands that cannot be supplied to node i at time t, namely the demand not served, i.e. DNS^{e}_{i} and DNS^{g}_{i}.

In this work, a simplified network-flow model is adopted, which quantifies the flow of commodities in the networks in and out nodes, respectively $f^{e}_{in,i}, f^{g}_{in,i}$ and $f^{e}_{out,i}, f^{g}_{out,i}$, and abstracts voltages in the power system and pressures in the gas system. Therefore, the transformer substations, located in the intermediate nodes from generators to consumers, and the compressor components along the gas network edges are neglected.

Finally, gas storage systems are modelled as intakes from gas terminals. The two infrastructure systems are coupled by gas-fired power plants, represented by the pair electrical generator and gas node. For generalization and simplification purpose, the power plant type and the details of the generation, transmission, storage and control are left to dedicated modeling for application to specific cases.

The needs of communities are modeled as pairs of electrical and gas demands, and are composed by the subset of N^{e}_{nodes} and N^{g}_{nodes} such that $D^{e}_{load,i} \neq 0$ or $D^{g}_{load,i} \neq 0$, and are indexed with $l = 1, \dots, N_{communities}$. This means that there could be communities with no gas demand, meaning, that they are totally based on electricity.

It is important to underline how the complexity of communities is neglected to consider them integrally from an energetic point on view, by reducing them to couples of electrical and gas demands. Nevertheless, the model could be improved with details on the community energetic strategy, by adopting an energy hub description [11,12,25] to be integrated with the multi-commodity network description, so to model community specific commodity generation, storage and dispatch. However, these considerations are beyond the modeling scope of this thesis.

3.2) Hazard Consequence on Networks

A simple stochastic model for the hazard consequence on the network is adopted. Network edges are assumed to be at nominal design capacity in the pre-event configuration. After the hazard occurrence they can either be healthy or totally disrupted. The network initial stochastic damage state is determined by performing independent random Bernoulli trials on each edge of all the commodity networks. If the edge suffers damage its capacity becomes 0, otherwise the capacity stays at its nominal value.

This strong assumption provides a simple and conservative starting point, by considering the worst case scenario for the edge if it sustains damage. The failure probability conditioned on the hazard occurrence is assumed 0.2 for power lines and 0.3 for gas pipelines. The high value is used to generate highly disruptive initial damage states.

This simple hazard model is aimed at creating initial damage configurations for testing the recovery model and is clearly not meant to be a high-fidelity representation of the damage states following hazards. A realistic generation of the initial damage configuration should include a data-driven damage estimation that integrates a stochastic model for the chosen hazard, the fragility model of the components and the spatially-distributed nature of the network [6,36]. Nevertheless, the development of such model goes beyond the scope of the present work. Furthermore, the failure of nodes is not considered but can be incorporated by the simultaneous failure of the edges connected to it.

3.3) Action Levels Formulation

Resilience can be achieved by implementing restorative and improvement measures on infrastructure system components. For simplification but without restricting the decision making on a specific a priori defined set of actions, a description in terms of action categories is proposed. The details on the actions to be performed in practice depend on the specific case study, and should be selected by the infrastructure stakeholders.

Following [31] and the resilience framework presented in Chapter 2, four action levels are introduced to map four categories of resilience actions to be implemented on the system edges. The four action categories are divided in two groups, i.e. pre-event actions, composed of *expansion* and *retrofit*, and post-event actions, composed of *resource availability* and *recovery*. The action levels and their meaning are summarized in Table 2.

The level of each action on each k^{th} commodity network j^{th} edge is characterized by an implementation cost t, $b_{k,j}^{\alpha}$ for expansion, $b_{k,j}^{\beta}$ for retrofit, $b_{k,j}^{\gamma}(t)$ for resource availability at time t and $b_{k,j}^{\lambda}(t)$ for response at time t. All the costs are proportional to the corresponding action level

Table 2: Resilience recovery action on system components and corresponding level details.

Action	Action Level	Meaning
Expansion	$\alpha_j^k \in [0,1]$	• Percentage of k^{th} commodity network j^{th} edge capacity expansion. • $\alpha_j^k = 1$: k^{th} commodity network j^{th} edge capacity expanded of 100% of its starting value.
Retrofit	$\beta_j^k \in [0,1]$	• Capability of k^{th} commodity network j^{th} edge of absorbing the hazard impact upon future occurrences. • $\beta_j^k = 0$: k^{th} commodity network j^{th} edge cannot sustain any hazard impact in future • $\beta_j^k = 1$: k^{th} commodity network j^{th} edge has full capability of sustaining a future hazard impact.
Resource Availability	$\gamma_j^k(t) \in [0,1]$	• Abundance for k^{th} commodity network j^{th} edge at time t of recovery and improvement resources after hazard impact. • $\gamma_j^k(t) = 0$: no available resources for resilience recovery of k^{th} commodity network j^{th} edge at time t. • $\gamma_j^k(t) = 1$: required resources for recovery and improvement of k^{th} commodity network j^{th} edge fully present and ready to be used at time t.
Response	$\lambda_j^k(t) \in [0,1]$	• Degree of recovery of k^{th} commodity network j^{th}edge during the recovery phase at time t • $\lambda_j^k(t) = 0$: repair phase at time t fails to recover k^{th} commodity network j^{th} edge functionality. • $\lambda_j^k(t) = 1$: repair phase at time t totally succeed in recovering the k^{th} commodity network j^{th} edge functionality.

and to the maximum cost for that action on the considered edge, b_{α}^{max} for expansion, b_{β}^{max} for retrofit, b_{γ}^{max} for resource availability, and b_{λ}^{max} for response. These lasts are considered constant and equal for each edge. Eq. (1)-(4) define the cost of each action on the j^{th} edge of the k^{th} commodity network.

$$b_{k,j}^{\alpha} = b_{\alpha}^{max}\alpha_j^k \tag{1}$$

$$b_{k,j}^{\beta} = b_{\beta}^{max}\left(1 + \alpha_j^k\right)\beta_j^k \tag{2}$$

$$b_{k,j}^{\gamma}(t) = b_{\gamma}^{max}\gamma_j^k(t) \tag{3}$$

$$b_{k,j}^{\lambda} = \left[b_{\lambda}^{max} - \left(b_{\lambda}^{max} - b_{\lambda}^{min}\right)\gamma_j^k(t)\right]\lambda_j^k(t) \tag{4}$$

The recovery timeframe is divided in $t = 1, \dots, N_t$ intervals considered as restoration phases. During each of them, the post-event recovery actions (*resource availability* and *recovery*) are deployed at variable intensity levels. On the other hand, the pre-event actions (*expansion* and *retrofit*) determine how the system sustains the hazard impact. Therefore no implementation time is associated to them because the decision to expand and retrofit capacity is taken before the occurrence of the hazard. Yet, these decisions are co-optimized together with the two post-event decisions during the simulation of the recovery process as detailed in Section 3.6. It follows that on each edge $M = 2 + 2N_t$ actions levels are associated.

3.4) Edge Capacity Recovery Process

The capacity of each edge is the maximum commodity flow it can transport. Therefore, the recovery of the edge functionality is equivalent to improving its capacity level by expanding and retrofitting it. The coordinated restoration of the edges' capacities is considered as the commodity network recovery from the hazard.

A flexible mathematical formulation for the capacity recovery, based on the action levels mapping defined in Section 3.3, has been proposed based on [31,33,40]. For each edge j of each commodity network k, let use denote $C_{k,j}^{nom}$ the pre-event, i.e. nominal, capacity,

$C_{k,j}^{dam}$ the post-event capacity, $C_{k,j}^{\beta}$ the retrofitted capacity and $C_{k,j}^{\alpha\beta}$ the retrofitted and expanded capacity, Eqs.(5)-(6) formalize the pre-event actions implementation and recovery objectives of each edge.

$$C_{k,j}^{\alpha} = C_{k,j}^{dam} + \beta_j^k \left(C_{k,j}^{nom} - C_{k,j}^{dam}\right) \tag{5}$$

$$C_{k,j}^{\alpha\beta} = C_{k,j}^{\beta}\left(1 + \alpha_j^k\right) \tag{6}$$

The dynamic restoration process is described by the response and resource availability action levels. Denoting by $C_{k,j}^{\alpha\beta,max}$ the maximum edge capacity attainable only by expansion and retrofit, and $C_j^k(t)$ the recovering capacity, a time dependent formulation is presented in Eq.(7).

$$C_j^k(t+1) = \begin{cases} \left(C_{k,j}^{nom} + C_{k,j}^{\alpha\beta}\right)\left[1 + \left(\frac{C_{k,j}^{\alpha\beta,max} - C_{k,j}^{dam}}{C_{k,j}^{\alpha\beta,max}}\right)\lambda_j^k(t)\left(1 - e^{-\gamma_j^k(t)}\right)\right] - C_{k,j}^{\alpha\beta} & if\ t = 0 \\ C_j^k(t)\left[1 + \left(\frac{C_{k,j}^{\alpha\beta,max} - C_j^k(t)}{C_{k,j}^{\alpha\beta,max}}\right)\lambda_j^k(t)\left(1 - e^{-\gamma_j^k(t)}\right)\right] & if\ t \geq 1 \end{cases} \tag{7}$$

A usual assumption in complex system restoration is to perform easier and less time consuming operations first [40], which is formalized by the negative exponential in Eq. (7). In the same equation, the ratio that weighs the exponential serves two purposes: i) it limits the growth of the capacity to $C_{k,j}^{\alpha\beta,max}$, which is equal to $2C_{k,j}^{nom}$ when $\alpha_j^k = \beta_j^k = 1$, and ii) imposes a priority strategy in the recovery of the edges. Indeed, if the edge did not sustain damage in the hazard event ($C_{k,j}^{dam} = C_{k,j}^{nom}$), then the ratio is smaller than for an edge that suffered damaged ($C_{k,j}^{dam} = 0$).

The limit to the capacity level is a direct consequence on action levels modeling assumptions, but it is reasonable in the context of electric power and gas infrastructure systems, as the installation of new lines are usually constrained by the high cost, the environmental impact and the total generation power.

Additionally, the expansion and retrofit influence is introduced in the first phase of the recovery process (t=0) through $C_{k,j}^{\alpha\beta}$, thus propagated along the entire recovery timeframe.

Therefore, the expansion and retrofit level, that defines the capacity maximum value and are co-optimized with recovery and resource availability actions as explained in Section 3.6, can be also considered as post-event restoration process objectives.

Resilience actions depend and are implemented within the time interval duration. This results in an exponential piecewise capacity recovery curve for each edge. An illustration of the recovery process is depicted in Fig.2.

Because the recovery of each edge happens simultaneously, the model also assumes that a dedicated repair crew can approach each damaged edge and, therefore, crew scheduling is not considered.

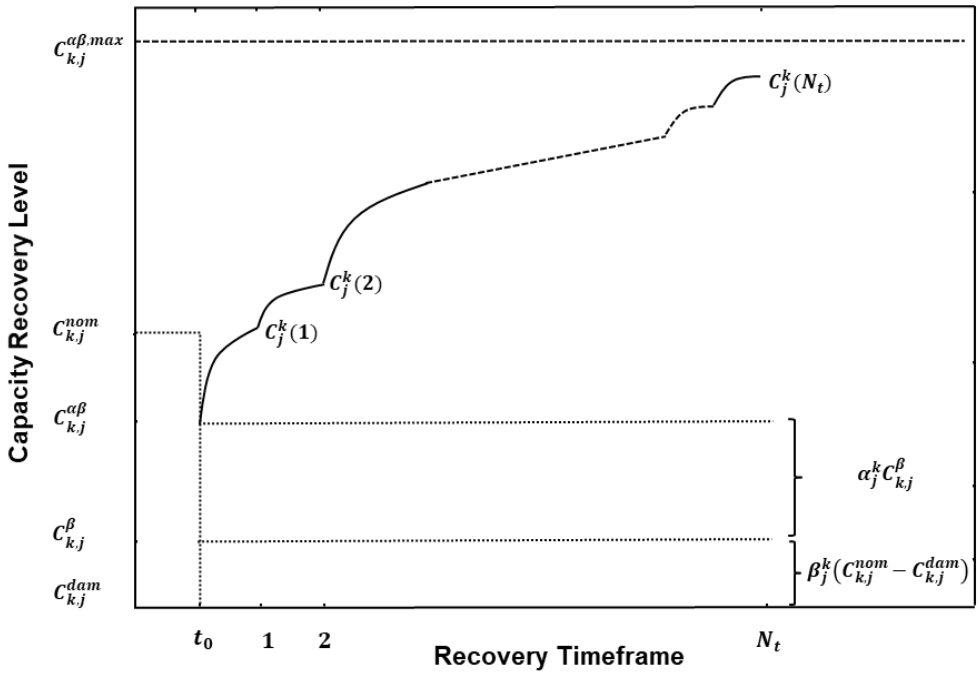

Fig.2: Edge capacity recovery process from the hazard occurrence at t_0, where the edge sustained a disruptive damage. The contribution of retrofit and expansion actions are represented by the straight dotted lines. The piece-wise exponential recovery is represented by the continuous line. The asymptote of the exponential curve is represented by the dashed line.

3.5) Network Flow Operation and Recovery Performance

The operations of the infrastructure systems described in Section 3.1 are modelled by the network flow programming modeling technique [4]. The proposed solution methodology relies on solving several constrained multi-period network flow problem [13,28].

The program for quantifying the operations of the flow commodity networks, minimizes the sum $z(t)$ of the total production cost and the overall unsatisfied demand costs for each commodities at time t, respectively. $z_e(t)$ and $z_g(t)$, i.e. Eq. (8) where $\eta_i^{P_e}$ and $\eta_i^{P_g}$ are the electrical and gas production cost of the generating unit located in the node i, under the constraints of network flow balance, Eqs. (9)-(10), line flow capacity, Eqs. (11)-(12), generation capacity, Eqs.(13)-(14), and demand not served limit to the load demand, Eqs.(15)-(16). The demand not served terms in Eqs. (9)-(10), to be minimized, give the system sufficient flexibility in the flow allocation.

$$min \;\; z(t) = z_e(t) + z_g(t) = \sum_{i=1}^{N_{nodes}^e} \left(\eta_i^{P_e} P_i^e(t) + \eta_i^{S_e} DNS_i^e(t)\right) + \sum_{i=1}^{N_{nodes}^g} \left(\eta_i^{P_g} P_i^g(t) + \eta_i^{S_g} DNS_i^g(t)\right) \tag{8}$$

$$\sum_{input\ edges} f_{in,\,i}^e(t) - \sum_{output\ edges} f_{out,\,i}^e(t) + P_i^e(t) - D_{load,i}^e + DNS_i^e(t) = 0\,, \;\; \forall\, i = 1, \dots, N_{nodes}^e \tag{9}$$

$$\sum_{input\ edges} f_{in,\,i}^g(t) - \sum_{output\ edges} f_{out,\,i}^g(t) + P_i^g(t) - D_{load,i}^g + DNS_i^g(t) = 0, \;\; \forall\, i = 1, \dots, N_{nodes}^g \tag{10}$$

$$0 \le \left|f_j^e(t)\right| \le C_j^e(t) = f(\alpha_j^e, \beta_j^e, \gamma_j^e(1), \gamma_j^e(1), \dots, \gamma_j^e(N_t), \lambda_j^e(N_t)) \qquad \forall\, j = 1, \dots, N_{edges}^e \tag{11}$$

$$0 \le \left|f_j^g(t)\right| \le C_j^g(t) = f\left(\alpha_j^g, \beta_j^g, \gamma_j^g(1), \lambda_j^g(1), \dots, \gamma_j^g(N_t), \lambda_j^g(N_t)\right) \quad \forall\, j = 1, \dots, N_{edges}^g \tag{12}$$

$$P_{min,i}^e \le P_i^e(t) \le P_{max,i}^e \quad \forall\, i = 1, \dots, N_{nodes}^e \tag{13}$$

$$P_{min,i}^g \le P_i^g(t) \le P_{max,i}^g \quad \forall\, i = 1, \dots, N_{nodes}^e \tag{14}$$

$$0 \le DNS_i^e(t) \le D_{load,i}^e \quad \forall\, i = 1, \dots, N_{nodes}^e \tag{15}$$

$$0 \le DNS_i^g(t) \le D_{load,i}^g \quad \forall\, i = 1, \dots, N_{nodes}^e \tag{16}$$

The performance of the networks during their resilient recovery is modelled also by network flow programming.

The performance of the network is quantified by the maximum aggregated flow/service that can be supplied to all communities, i.e. by Eq.(17) where $D_l^k(t)$ is the k^{th} commodity demand that can be supplied to community l at time t. Before the hazard occurrence the commodity k network is supplying the load demand to each node i, i.e. $D_{load,i}^k$; the hazard causes damage on the network such that the load demand may not be satisfied and a demand not served of commodity k to node i, i.e. DNS_i^k, is generated; as the network is recovered the allowable demand of commodity k to community l, $D_l^k(t)$, changes. The higher the total commodity flow that could possibly reach communities, the more efficient the network recovery.

Therefore, the maximum allowable demand in the community nodes provides a quantification of the capability of the recovered transmission infrastructure to transmit the service and it is used as a resilience performance measure of the network recovery [27]. The corresponding objective function is described in Eqs.(17), solved under the constraint in Eqs. (18) to (24), which are similar to the aforementioned constraints Eqs. (9)–(16).

$$max \sum_{l=1}^{N_{communities}} D_l^k(t) \qquad \forall k\ commodity \tag{17}$$

$$\sum_{input\ edges} f_{in,i}^e(t) - \sum_{output\ edges} f_{out,i}^e(t) + P_i^e(t) - D_i^e(t) = 0\ ,\ \ \forall\ i = 1, \dots, N_{nodes}^e \tag{18}$$

$$\sum_{input\ edges} f_{in,i}^g(t) - \sum_{output\ edges} f_{out,i}^g(t) + P_i^g(t) - D_i^g(t) = 0,\ \ \forall\ i = 1, \dots, N_{nodes}^g \tag{19}$$

$$0 \le \left|f_j^e(t)\right| \le C_j^e(t) = f\left(\alpha_j^e, \beta_j^e, \gamma_j^e(1), \gamma_j^e(1), \dots, \gamma_j^e(N_t), \lambda_j^e(N_t)\right) \qquad \forall\ j = 1, \dots, N_{edges}^e \tag{20}$$

$$0 \le \left|f_j^g(t)\right| \le C_j^g(t) = f\left(\alpha_j^g, \beta_j^g, \gamma_j^g(1), \lambda_j^g(1), \dots, \gamma_j^g(N_t), \lambda_j^g(N_t)\right) \quad \forall\ j = 1, \dots, N_{edges}^g \tag{21}$$

$$P_{min,i}^e \le P_i^e(t) \le P_{max,i}^e \quad \forall\ i = 1, \dots, N_{nodes}^e \tag{22}$$

$$P_{min,i}^g \le P_i^g(t) \le P_{max,i}^g \quad \forall\ i = 1, \dots, N_{nodes}^e \tag{23}$$

$$D_l^k \ge 0 \quad \forall l\ community, \forall k\ commodity \tag{24}$$

3.6) Cooperative Coevolution and Decision Making of the Communities

An agent-based approach is adopted for modeling communities' decision making. To this aim, agent l is responsible for community l and, during the recovery of the network, pursues the objective of maximizing the resilience of community l, i.e. maximizing the demand for each commodity k to community l:

$$max\ D_l^k\ (t) \qquad \forall k\ commodity \tag{25}$$

Due to the budget conflict between the restoration of the shared infrastructure and the provision of local buffers/resources, the optimal recovery solution, that is the action levels set on the network edges, i.e. the $N_{edges}^k \times M$ matrix S_k such that $s_1^{j,k} = \alpha_j^k,\ s_2^{j,k} = \beta_j^k,\ s_3^{j,k} = \gamma_j^k(1),\ s_4^{j,k} = \lambda_j^k(1), \dots,\ s_{M-1}^{j,k} = \gamma_j^k(N_t),\ s_M^{j,k} = \lambda_j^k(N_t)$ for each edge j of the k^{th} commodity network, may be conflicting for each community l. Therefore, an abstract agent representing the overall benefit of the communities, called the transmission system operator (TSO) agent, is introduced to seek accordance among the different community agents' objectives. The TSO agent's objective is the maximization of the resilience performance of the network recovery which is measured, as described in Section 3.5, by the maximization of the allowable demand to all communities, i.e. by Eq. (17).

Each agent objective is a possible objective function for the optimization of the recovery solution. Therefore, contrasting different agents' decision is equivalent to comparing the corresponding optimized action levels set.

The high level of non-linearity of the edge capacity update in Section 3.4 poses great analytical and computational challenges to classic program optimization methods [22,33]. Coupled with the multi-objective nature of the problem, a Cooperative Coevolution (CC) approach is adopted [21,26]. Following [21], the CC is used as metaheuristics, with which to contrast recovery solutions optimized with respect to different agent's heuristics.

A Differential Evolution (DE)-based method is used as recovery solution optimization tool [35], and the following iterative procedure, called *DE step*, is used to avoid a greedy algorithm paradigm:

1. The action level set is defined as the $N_{edges}^{k} \times M$ matrix where each row is composed by the action level set on the j^{th} edge along the entire recovery timeframe for each commodity k.

2. The action level set thus defined is used as an individual to be evolved through the DE. A population of N_{pop} individuals is initialized, by randomly sampling each action level.

3. The DE optimization is carried on for N_{DE} iterations as follows:

   3.1. The starting individual of the population is selected and mating, crossover and mutation rules of a standard DE are used to generate a new candidate individual.

   3.2. The edge capacities are computed with Eqs. (5)-(7), using the new candidate solution, for all recovery time steps and used as parameters in the optimization programs flow constraints, i.e. Eqs.(11), (12), (20) and (21).

   3.3. For each $t = 1, \dots, N_t$:

      3.3.1. Eq. (17) for the optimization of the TSO agent or Eq. (25), for the optimization of the communities' agents, based on the considered heuristic during the methodology algorithm, is solved under the constraints Eqs. (18)-(24) to determine $D_l^k(t)$ for each community l and commodity k.

      3.3.2. Eqs. (8)-(16) is solved to determine $DNS_l^k(t)$ for each community l and commodity k.

      3.3.3. The action level set is used to update again the edge capacities determined in 3.2. The community makes in this way a prediction on the network recovery state in the next time step, i.e. $t + 1$, by projecting the recovery solution at time t in the following time step.

      3.3.4. Eqs. (8)-(16) are solved using the capacities computed in 3.3.3 to determine the projected demand not served in the next time step, i.e. $DNS_{proj,l}^k(t)$, for each community l and commodity k.

      3.3.5. To quantify the community contribution to the recovery of the infrastructure system, the community participation at time t, i.e.$p_l^k(t)$ defined in Eq. (26) is introduced for each community l and commodity k. The higher $p_l^k(t)$ the more the community l invest in the recovery of the k^{th} commodity network at time t.

3.3.6. The cost of the candidate action level set is determined by solving Eq. (1)-(4) for each community l and commodity k.

3.3.7. The total budget allocated to the recovery of the k^{th} infrastructure at time t, i.e. $B^k(t)$, is determined from Eq. (27), where B^k_{max} is the maximum recovery budget for the k^{th} infrastructure and $w^k_l(t)$ the demand load of commodity k of community l normalized on the total demand load of commodity k, i.e. $D^k_{load,l} \Big/ \sum_{l=1}^{N_{communities}} D^k_{load,l}$.

3.4. The $D^k_l(t)$ for each commodity k and community l determined at point 3.3.1 are combined in the fitness function f, i.e. Eq. (28), where $D^k_{l,max,nom}$ is the maximum allowable demand of commodity k to community l in the pre-event network condition. It represents the resilience performance of the recovery solution with respect to the performance in the undamaged network condition. In order to consider the budget constraint on the recovery actions implementation and the reduction of the demand not served to communities, the fitness function f is penalized, i.e. ϕ defined in Eq. (31), by subtracting the budget constraint penalty for each commodity k, i.e. h_k defined in Eq. (29), and demand not served constraint penalty for each commodity k, i.e. l_k defined in Eq. (30), both weighed with a penalization factor, i.e. η^{h_k} and η^{l_k} respectively, tuned experimentally [7].

3.5. If the function ϕ evaluated for the candidate individual is higher than for the starting one, the candidate solution substitute the starting individual in the population. In the opposite case the candidate solution is discarded.

3.6. Steps 3.1 to 3.5 are repeated for each individual of the population.

4. The candidate with the largest ϕ in the population after N_{DE} iterations is considered as the set of optimized action levels for the communities agents if the objective function used in 3.3.1 is Eq. (25) or for the TSO agent if the objective function in 3.3.1 is Eq. (31).

$$p^k_l(t) = e^{-\left(\frac{DNS^k_l(t)}{D^k_{load,l}} + \frac{DNS^k_{proj,l}}{D^k_{load,l}}\right)} \tag{26}$$

$$B^k(t) = \sum_{l=1}^{N_{communities}} p^k_l(t) w^k_l B^k_{max} \tag{27}$$

$$f = \sum_{t=1}^{N_t} \sum_{l=1}^{N_c} \sum_k \frac{D^k_l(t)}{D^k_{l,max,nom}} \tag{28}$$

$$h_k = \sum_{T=1}^{N_t} \left[\sum_{t=1}^{T} \left(\sum_{j=1}^{N^k_{edges}} b^{\alpha}_{k,j} + b^{\beta}_{k,j} + b^{\gamma}_{k,j}(t) + b^{\lambda}_{k,j}(t) \right) - B^k(T) \right] \tag{29}$$

$$l_k = \sum_{t=1}^{N_t} \sum_{l=1}^{N_{communities}} DNS_l^k(t) - D_{load,l}^k \quad (30)$$

$$\phi = f - \sum_k \eta^{h_k} h_k + \eta^{l_k} l_k \quad (31)$$

Because *DE step* bases a present decision on the prediction of the future, it introduces a self-fulfilling prophecy dynamics for the community partecipation. Moreover, communities' decisions have a positive feedback on the decision of the others, given that the variation of total available budget directly influences each community via the recovered performance of the shared infrastructures. To achieve a trade-off solution between different objectives, the following iterative procedure, called *conversation step*, is carried on:

a. Perform the *DE step* for the TSO agent, i.e. perform Step 1 to 4 of the iterative procedure above using Eq (17) at Step 3.3.1, and determine the TSO agent recovery solution.

b. Perform the *DE step* independently for each community agent heuristic using the TSO agent solution for the capacities, i.e. perform Step 1 to 4 of the *DE step* iterative procedure using Eq. (25) as the objective function at Step 3.3.1 for each community l, using the TSO agent solution as starting solution at Step 2, and determine the communities' agents recovery solutions.

c. Determine the community agent recovery solution with the highest fitness function ϕ, called *conversation leader*.

d. Compare each l^{th} community agent solution with the conversation leader solution, by checking whether if the action levels of the former are within a $\pm\rho$ range from the latter. Generate the $N_{edges}^k \times M$ *occurrence matrix* $O_k = [o_m^{j,k}]$ such that, defined $q_m^{j,k}$ the conversation leader m^{th} action level on the edge j of the k^{th} commodity network, where $m = 1, \dots, M$, and defined $\delta_m^{j,k}(l) = \begin{cases} 1 \; if \; s_m^{j,k}(l) = q_m^{j,k} \\ 0 \; if \; s_m^{j,k}(l) = q_m^{j,k} \end{cases}$, the element $o_m^{j,k} = \sum_{l=1}^{N_C} \delta_m^{j,k}(l)$.

e. For each edge j of the k^{th} commodity network, if $o_m^{j,k} \geq \frac{N_{communities}-1}{2}$, then all communities adopt the leader action level in that position for the edge j, i.e. $s_m^{j,k,l} = q_m^{j,k}$. This is equivalent to saying that the communities adapt to the leader if the majority is in accordance with the leader.

f. Perform again the *DE step* independently for each community agent objective using the new candidate action level matrixes as new starting recovery solutions, i.e. perform Step 1 to 4 of the *DE step* iterative procedure using Eq. (25) at Step 3.3.1 for each community l using the candidate solutions determined at Step e as starting point for the iterations, and determine the new candidate communities' agents recovery solutions.

g. Repeat from Step c.

h. After N_{COOP} iterations, the next conversation leader solution is taken as cooperative coevolution recovery solution, which represents the communities' trade-off solution.

The CC algorithm seeks for an accordance, i.e. cooperation, between different agents' recovery solutions, which are optimized with an evolutionary algorithm, i.e. coevolution. The high level flowchart of the algorithm is presented in Fig.3. Starting from a network damage state scenario, the DE step for TSO objective and communities' objective is performed. The conversation step is carried on and the outcoming communities' trade-off solution is once again re-optimized with respect to the TSO agent objective. After N_{CC} iterations the TSO agent solution is accepted as network resilient recovery solution. While the algorithm forces the communities most in disagree to accept the leader solution, the entire optimization is iteratively guided by the demand not served and recovery performance of the network. Therefore, trade-off solutions with low performance and high community disservice, i.e. recovery solutions that do not fully supply the load demand to each community, are discarded.

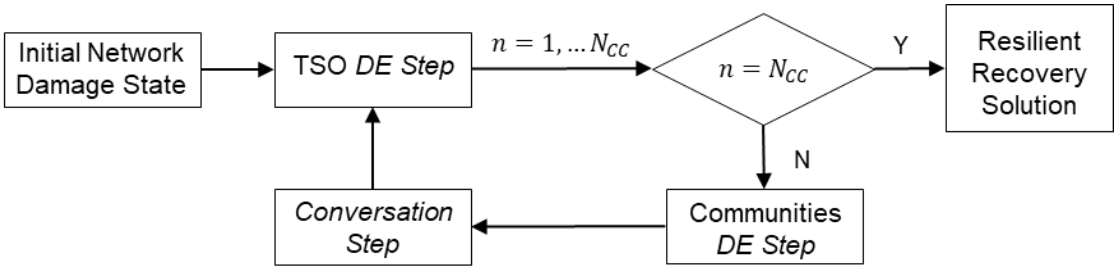

Fig.3: Cooperative Coevolution (CC) flowchart.

Chapter 4

Applications and Results

4.1) Case Study

The methodology is tested on a small benchmark network of *Fig.4* [38]. The interdependence of the 6 nodes and 7 edges power grid and the 7 nodes and 6 edges gas network is through the G2 and G3 Gas Fired Power Plants (GFPP).Three communities are considered by pairing the electric and load demands as follows: ($D^{e}_{load,1}$, $D^{g}_{load,1}$), ($D^{e}_{load,2}$, $D^{g}_{load,2}$) and ($D^{e}_{load,3}$, $D^{g}_{load,3}$).

For representation purposes, the optimization horizon for the recovery is set to one month, and $N_t = 4$ time steps are considered. All the remaining quantities are summarized in Table2, together with the solution model parameters. The total maximum budget depends on the maximum action budget and computed as: $B^{k}_{max} = N^{k}_{edges}\left(b^{max}_{\alpha} + b^{max}_{\beta} + b^{max}_{\gamma} + b^{max}_{\gamma}\right)$ for each k commodity.

Table 3: Solution methodology parameters.

b^{max}_{α}	0.01	$Mln\$$
b^{max}_{β}	0.01	$Mln\$$
b^{max}_{γ}	0.1	$Mln\$$
$\left[b^{min}_{\lambda}, b^{max}_{\lambda}\right]$	$[0, 0.1]$	$Mln\$$
B^{e}	1.54	$Mln\$$
B^{g}	1.32	$Mln\$$
η^{h_e}, η^{h_g}	0.05	$1/Mln\$$
η^{l_e}	10^{-5}	$1/MW$
η^{l_g}	10^{-5}	$1/(m^3/s)$
N_{CC}	10	-
N_{COOP}	5	-
ρ	0.05	-
N_{pop}	5	-
N_{DE}	10	-
(F_{min}, F_{max})	$(0.2, 0.8)$	-
$P_{crossover}$	0.9	-

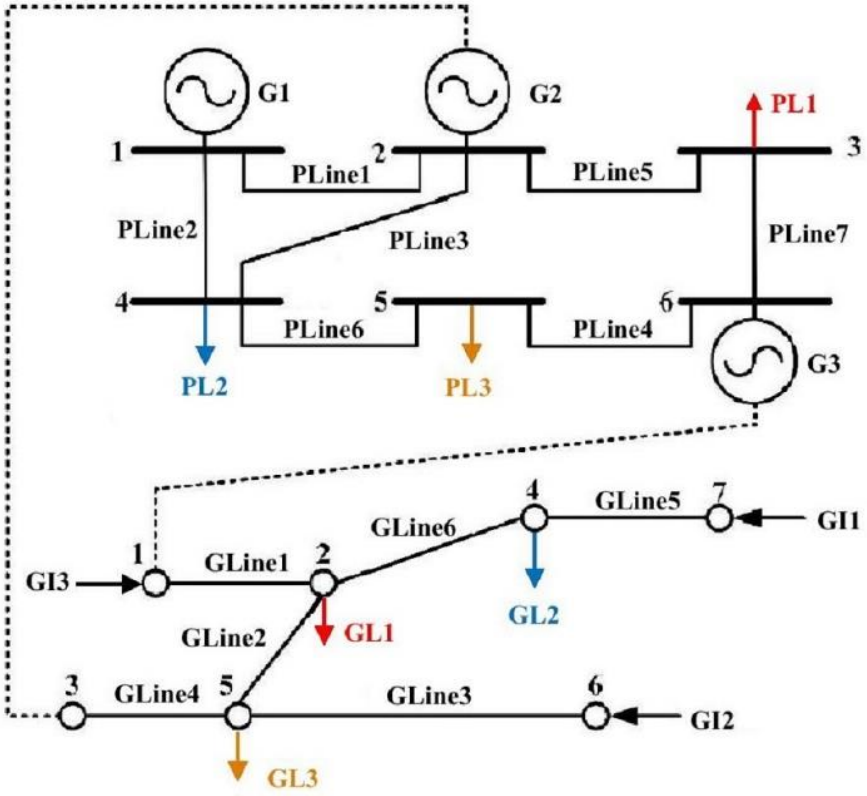

Fig.4: Benchmark case study network scheme. G: electricity generators, GI: gas imports, PLine: power grid edge, GLine: gas network edge, PL: electricity load, GL: gas load. Three communities are considered: (PL1,GL1) in red, (PL2,GL2) in blue, (PL3,GL3) in yellow.

4.2) Network Disruption and Recovery

The network restorations from the disruptive scenario, represented in *Fig.5,* are used throughout chapter 4 to illustrate the results.

The loss of PLine1 and PLine2 completely isolates the power plant G1 from the network. Due to the loss of GLine2 and GLine3 also the gas fired unit G2 is disconnected. Therefore, a large DNS_2^e and DNS_3^e are expected, whereas $D_{load,1}^e$ (PL1) is satisfied by the unit G3. As for the gas network, only $D_{load,1}^g$(GL1) can be satisfied, whereas the other two communities suffer from the disconnection of the gas terminals GI1 and GI2. The restoration is expected to concentrate on recovering the broken edges that assure the commodity injection in the network, namely PLine1, PLine2, GLine3 and GLine5.

The reduced dimensionality and complexity of the network, allows to focus on the resilient recovery rather than the complex dynamics of the system, making it easier to compare the expected results with the ones from the methodology. The CC algorithm is implemented and solved using MATLAB software and the linear programs of Section 2.5 are solved employing GUROBI [13] via YALMIP [19]. The results are obtained running the simulation on the EULER cluster at ETH Zurich. The computational time was 11576 seconds.

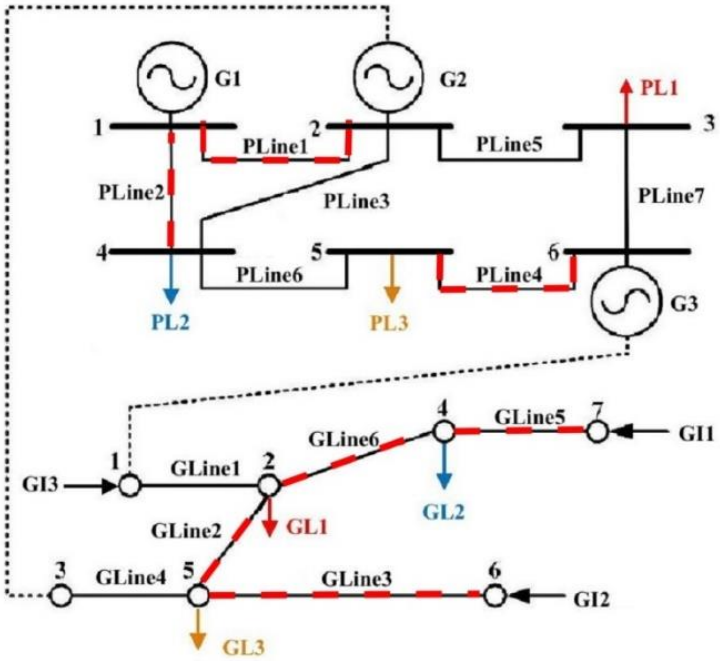

Fig.5: Highly disruptive initial damage state.

4.3) Network Damage Absorptive Capability

The recovered network in the four weeks is depicted in Fig.6. From Fig.6, it is clear how the methodology is capable of considering the hazard impact absorptive capability of the network, as both recovery of disrupted edges and strengthening of healthy ones are carried on. Therefore, the proposed model can restore the network functionality by avoiding the recovery of the disrupted edges and improving the surrounding ones.

As expected, the CC algorithm moves in the direction of restoring the connections of communities to generators. A great effort is put on PLine1 directly from the first time iteration.

On the other hand, instead of focusing on the recovery of PLine2, PLine3 is strengthened, together with PLine5 towards community 1 and PLine6 towards community 3. This implies a greater reliance on gas-fired generator G2. Coherently, the path from G2 to the closest gas import GI2 is reinforced. In particular, the greater effort on GLine4 than on GLine3 is justified by its nominal capacity of the being almost four times lower than the latter.

Therefore, the algorithm shows the feature of being able to find alternative network configurations to satisfy community loads. The same can be observed in the gas network. Recovering PLine4 would support the electric supply to community 3, which is, however, also supported by generator G2 owing to the improvement to PLine6. Nonetheless, the converged solution does not include the recovery of PLine4 and, therefore, the gas import from GI3 is used to supply the gas demand of Community 1 and 2 instead of being converted into electricity in GFPP G3. Therefore, the method recovers and strengthens GLine6 more favorably than GLine5, having a lower capacity, and improves GLine1 to guarantee the gas flow from GI3. Once again, the recovery of the disrupted edge GLine2 is bypassed.

In the last week, all three gas imports are reconnected. Indeed, GLine3 is recovered up to its nominal capacity, GLine5 is recovered almost up to its nominal capacity and GLine1 is strengthened. Thus, all the electrical generators and gas imports are reconnected to the communities in the considered recovery timeframe. The algorithm gives up the recovery of the redundant line Gline2 because of its nominal capacity, which is three times higher than the nominal capacity of GLine4, the most strengthened line. The same can be said for the strengthening of the path Pline7-Pline5-Pline3-Pline6 to community 3 rather than the recovery of Pline4 from the generator G3.

It can be concluded that the algorithm tends to strengthen all the edges which nominal capacity is lower, while being guided by the optimization of total allowable demand as resilient recovery performance measure, constrained by the minimization of the total disservice to the communities.

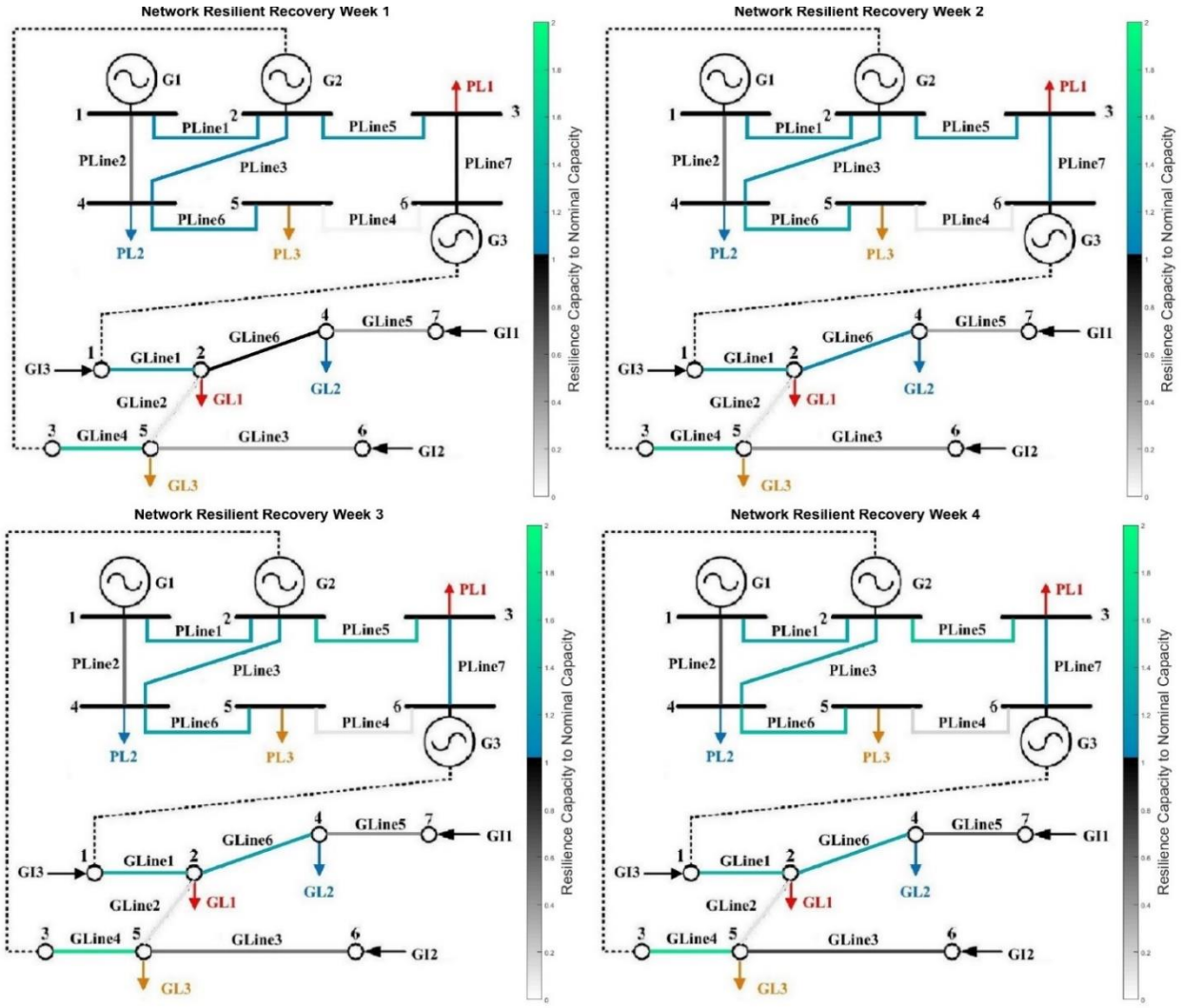

Fig.6: Network resilient recovery. The ratio of the edge recovered capacity to the edge nominal capacity is plotted on the network for each edge in each recovery time step. A white to black color bar is used for recovery up to nominal capacity, whereas a blue to green one for the strengthening of the edge above its nominal capacity.

4.4) Resilience Performance and Coordination Feature

Figs.7 and 8 show the maximum demand that could be supplied to each community and the demand not served for each community during the recovery time horizon at the N_{CC} (last) iteration of the methodology.

The results of Fig.8 demonstrate that the penalization term with respect to the demand not served in Eq. (30) constraints the demand not served of each community to decrease to zero. The cooperative coevolution is guided by the penalized fitness function in Eq. (31), which cumulates the maximum demand supplied to each community. Therefore, the maximum demand that could be supplied to a community, e.g. the demand of electricity for Community 1 and 3 in Fig.7, can decrease in favor of the increase of the maximum demand of another community, i.e. the demand of electricity for Community 2 in Fig. 7, if this entails an overall gain in network recovery performance.

In Fig.7, the maximum allowable electrical demand to Community 3 and the maximum allowable gas load demand to Community 2 decrease to zero. For the former, this is justified by the fact that the recovery of the edges PLine1, PLine2 and PLine3 contribute first to satisfy the load demand of Community 2, being closer to the generators G1 and G2 than Community 3. The performance of the recovery solution is thus higher for Community 2 than for Community 3, as can be verified by the curve in Fig.7. Community 3 benefits from the recovery of the surrounding network driven by Community 2, as the connections to the generators are restored. The strengthening of PLine6 edge that connects Community 2 to Community 3 serves to satisfy the load demand of Community 3. Moreover, the fact that PLine4, a redundant supply line, is not recovered makes Community 3 contribution to the recovery of the electric power network even less important. The same justification is valid also for maximum allowable gas demand to Community 2. The recovery of the gas network is driven by Community 1 and 3, as can be verified by the increasing maximum allowable gas demand to Community 1 and maximum allowable gas demand to Community 3 in Fig. 7. The strengthening of GLine6 is to satisfy the load demand to Community 2 to compensate the loss of supply line GLine5.

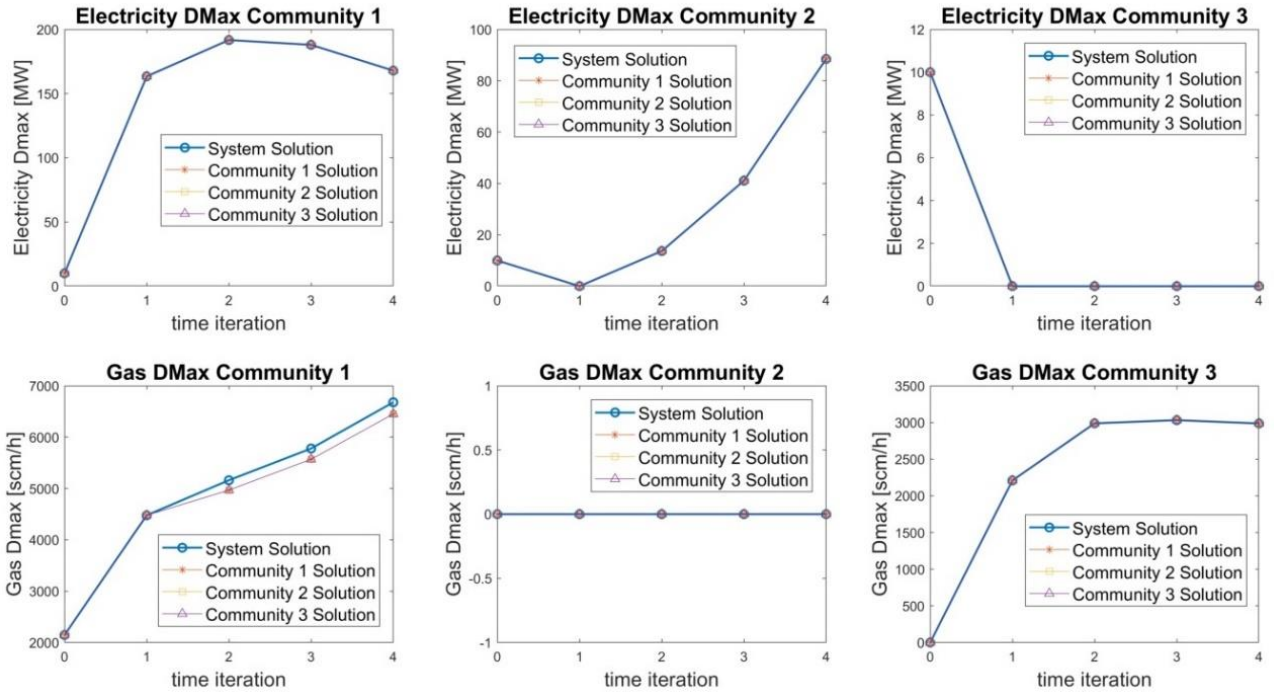

Fig.7: Max allowable electric and gas demand to community nodes results for TSO (System) and community metaheuristics, at the last iteration of the methodology.

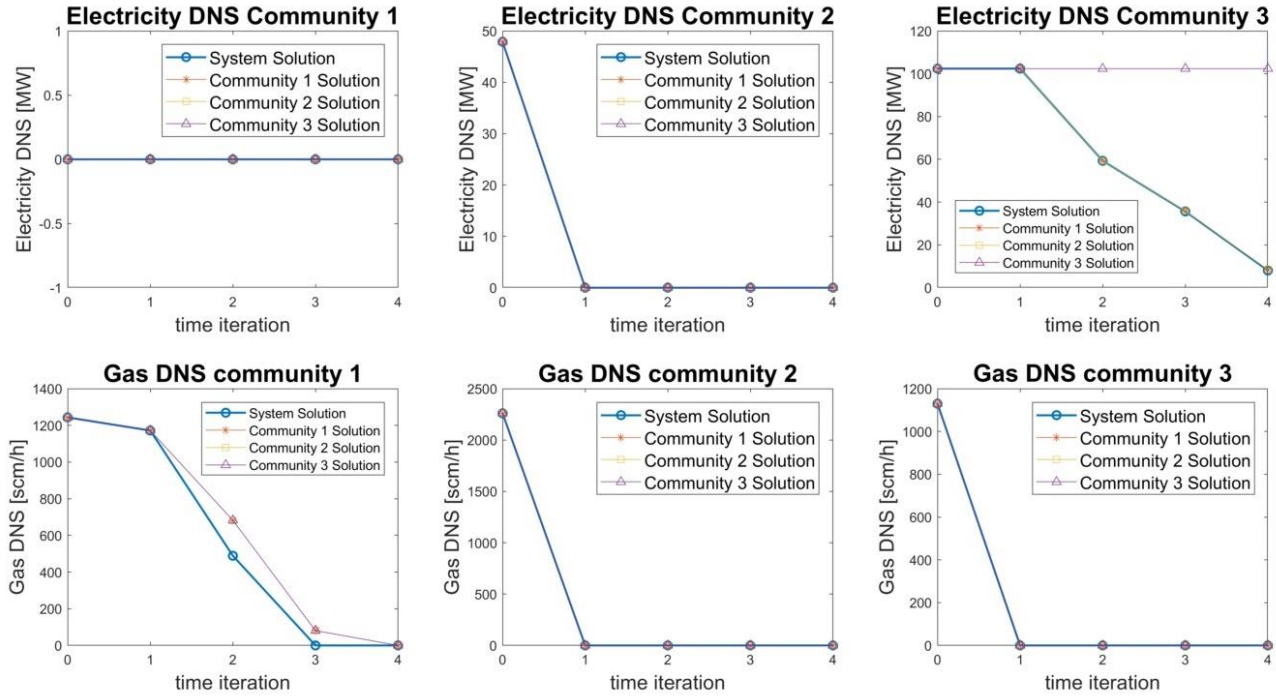

Fig.8: Electrical and gas demand not served of community nodes results for TSO (System) and community metaheuristics, at the last iteration of the methodology.

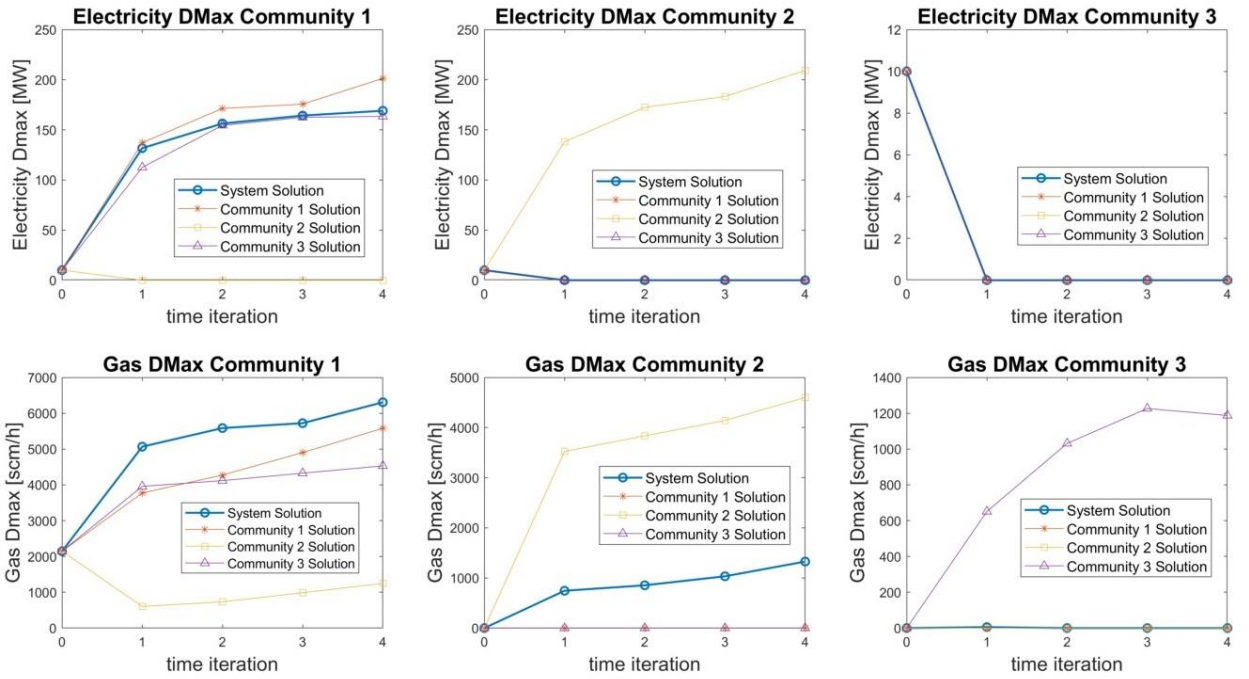

Fig.9: Max allowable electric and gas demand to community nodes results for TSO (System) and community metaheuristics, at the first iteration of the methodology.

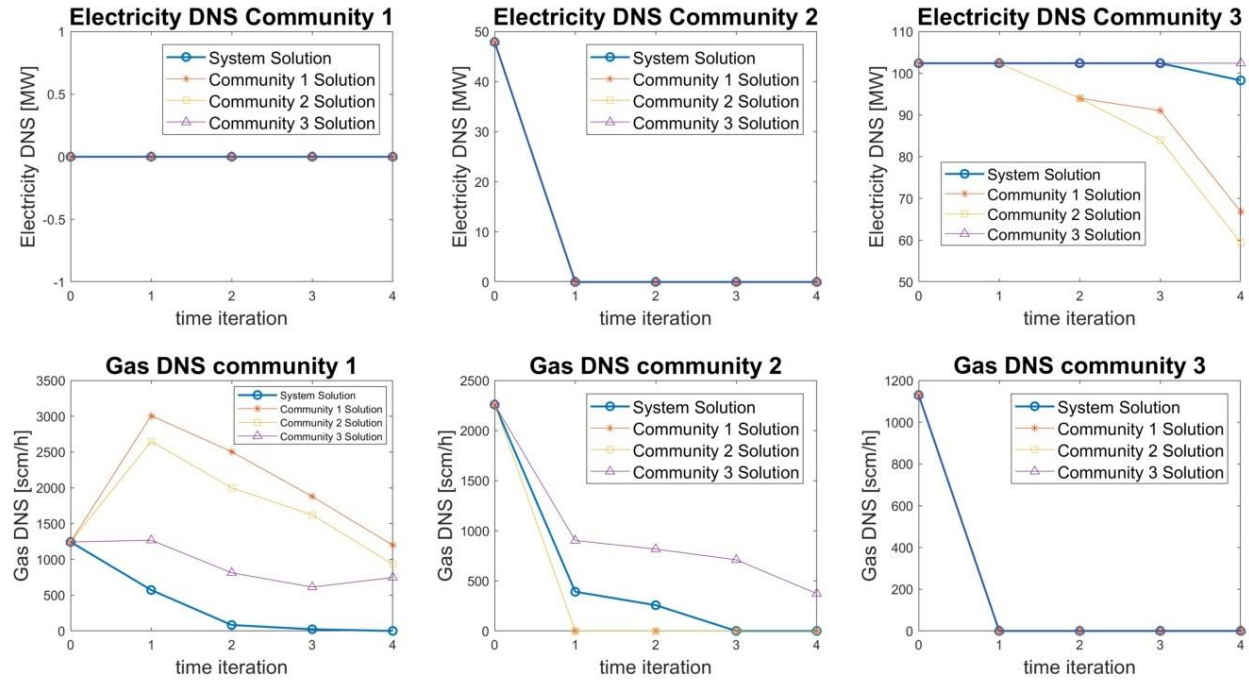

Fig.10: Electrical and gas demand not served of community nodes results for TSO (System) and community metaheuristics, at the first iteration of the methodology.

Fig.9 and Fig.10 show the maximum demand that can be supplied to each community and the demand not served for each community at the first iteration of the methodology.

The comparison of Fig.7-8 with Fig.9-10 demonstrates the coordination capability of the TSO and of the community agent objectives. In the first iteration of the methodology, Community 2 proposes a solution that maximizes both the electric and gas allowable demand to Community 2 at the expense of Community 1 and 3 in Fig.9, while Community 1 and 3 propose a solution that decreases maximum electric allowable demand to Community 2 to zero. All communities are in discordance in the gas network, mutually proposing recovery solutions that increase their maximum demand that could be supplied to each community at the expenses of the others. Nonetheless, Community 3 is in the proximity of Community 2 in the electrical power network, and, therefore, it benefits from the solution for Community 2. Community 3 is also topologically sequential to Community 2 and most of the electricity is supplying Community 2 first, and this causes a high DNS_3^e, as can be seen in Fig.10. Moreover, the recovery solution proposed by Community 2 in the first iteration of the methodology is also the one contributing the most to the decrease of DNS_3^e, as can be noted by the yellow line in Fig.10. Community 3 benefits from the recovery of the network for Community 2, and, therefore, in the last iteration of the methodology the tradeoff solution is more inclined to follow Community 2 and 1, as can be noted by the maximum electric allowable demand to Community 2 and 1 in Fig.7, and the methodology is favorable to mildly decrease the effort to Community 1 to focus on Community 2, as it can be noted by the slight decrease of the maximum electric allowable demand to Community 1 in favor of the maximum electric allowable demand in Fig.7. In the gas network, all communities are in competition for accessing to gas import GI3, which is the only one still connected to the network after the hazard occurrence. Community 2 is topologically sequential to Community 1, which is the closest to gas import GI3, and, therefore, it benefits from the recovery of the gas network for Community 1. Community 3 is directly connected through GLine4 to the gas-based generator G2, which is fundamental for the recovery of the electrical power network for all communities, as can be noted from Fig.6. The recovery of the gas network for Community 3 directly influences the gas supply to the generator G2. Therefore, the methodology in the last iteration is more inclined in following Community 1 and 3 for the gas network recovery, as can be noted in Fig.7.

At the last iteration, the network recovery solutions for all communities overlap with the TSO solution in Fig.7. This has several justifications. First of all, the heuristics objectives, i.e. Eq. (25) for each community l and Eq. (17) for the TSO agent, are not so much different from

each other. They are all related to finding the network configuration that maximizes the network capability of supply the demand nodes. Second, as described in Section 3.6, the algorithm proceeds such that all communities iteratively compare, optimize and evaluate their solutions. Third, the small size of network is such that it is very likely that the same network configuration and edges recovery strategy that is optimal for one community is also close to optimal for the other communities.

Finally, the comparison of Fig.8 and Fig.10 shows how in the last iteration of the methodology the demands not served are equal or lower than in the first iteration in each recovery phase. This is a due to the demand not served penalization, i.e. Eq. (30) to the fitness function, i.e. Eq. (31). The methodology iteratively finds a trade-off solution with a higher fitness function, thus with a lower demand not served to each community.

4.5) Network Recovery Configurations from Independent Runs

Starting from the initial damage state in Fig. 4, the recovery methodology is tested on $N_k = 50$ independent runs. As the penalized fitness function ϕ, Eq.(31), has been considered as network recovery performance for the communities, the penalized fitness value at the last iteration of the methodology is used as parameter to rank the solutions. The three highest fitness solutions are compared in this chapter and are represented in Figs. 11, 12 and 13. In all of the cases, the recovery of the electric network is similar, where the recovery of the edges PLine1, PLine3 and PLine5 is prominent. The most evident difference is on PLine4 which degree of recovery is directly related to the restoration of the gas network, as it impose a higher gas supply to the generator G3. The biggest difference is about the recovery of the gas network. The third highest fitness solution in Fig.11 shows a disconnected network, as the closest connections between the gas imports and the communities are strengthened at the expense of the connections between them. The second highest fitness solution in Fig. 12 and especially the first highest fitness solution in Fig. 13 shows a more connected and strengthened network by reducing the effort on GLine4 and GLine1. The methodology is thus capable of exploring different competitive trade-off solutions able to satisfy the communities' load demands and maximize the total maximum allowable demand.

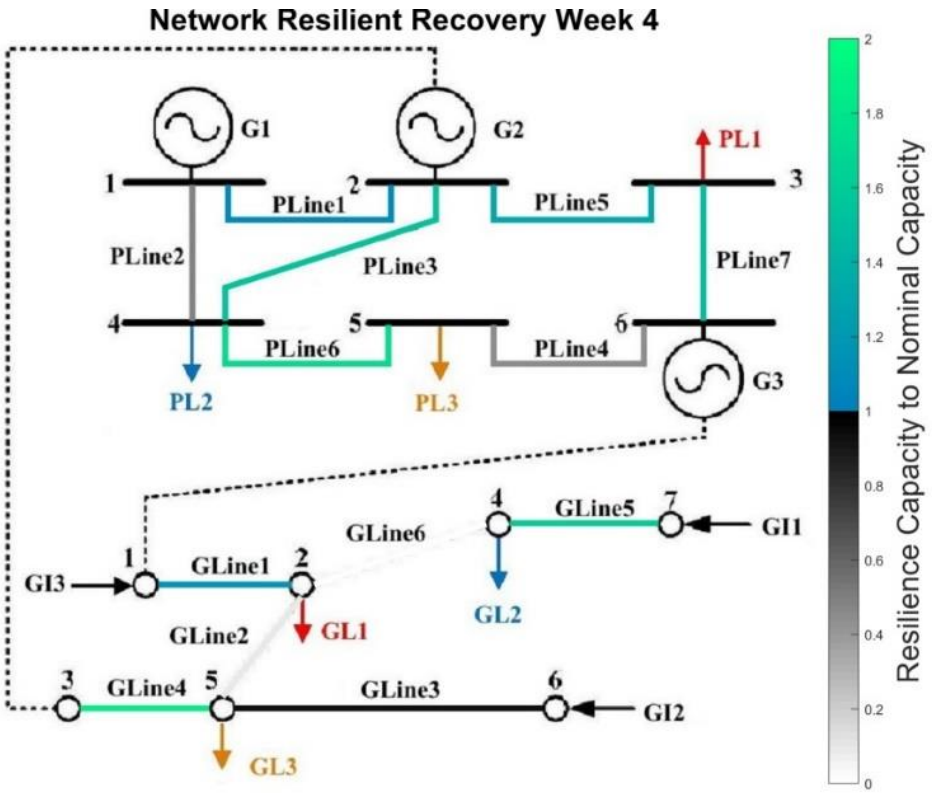

Fig.11: Third highest fitness recovery solution.

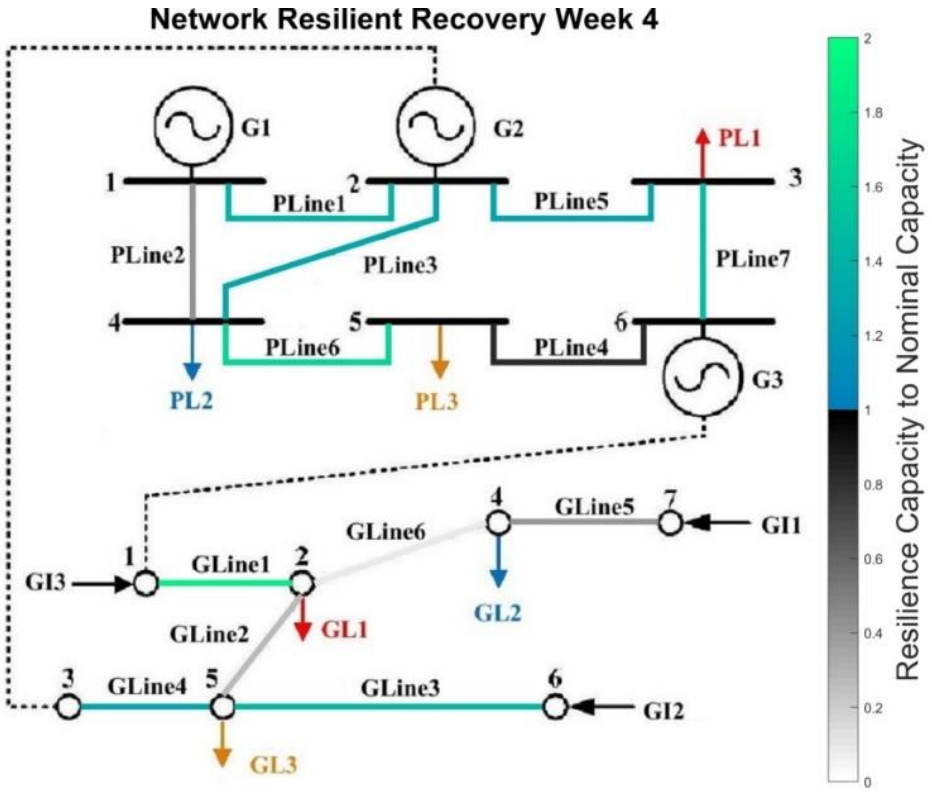

Fig.12: Second highest fitness recovery solution.

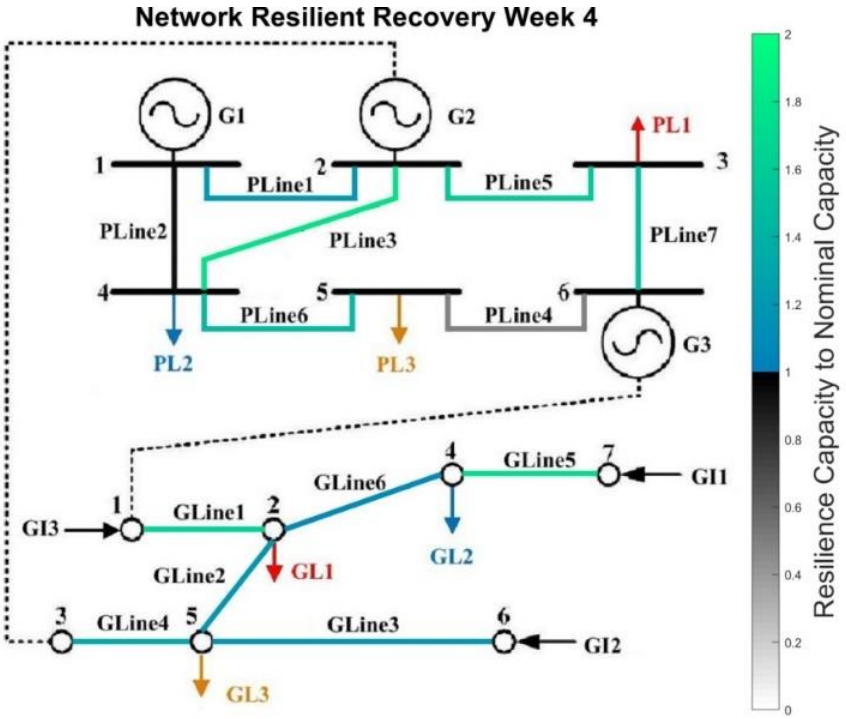

Fig.13: First highest fitness recovery solution.

4.6) Scalability of Methodology

The methodology is also tested on the benchmark case study of Fig. 14 [38]. It is composed of the interdependent 39 nodes electric power network and 20 nodes gas network, representative of the Belgian gas network, which are connected by three gas fired power plants. The first 9 communities are considered by coupling electric and gas load demands, while the remaining 9 communities are represented only by the corresponding electric nodes, meaning that they are assumed to rely solely on electricity to sustain their functionalities. The dataset and the level of details on the network are similar to the previous case study. Therefore, no spatial details or specific constraints are used in the following analysis, and the application of the recovery methodology is to investigate the scalability and the coherency of the results when applied to a bigger network.

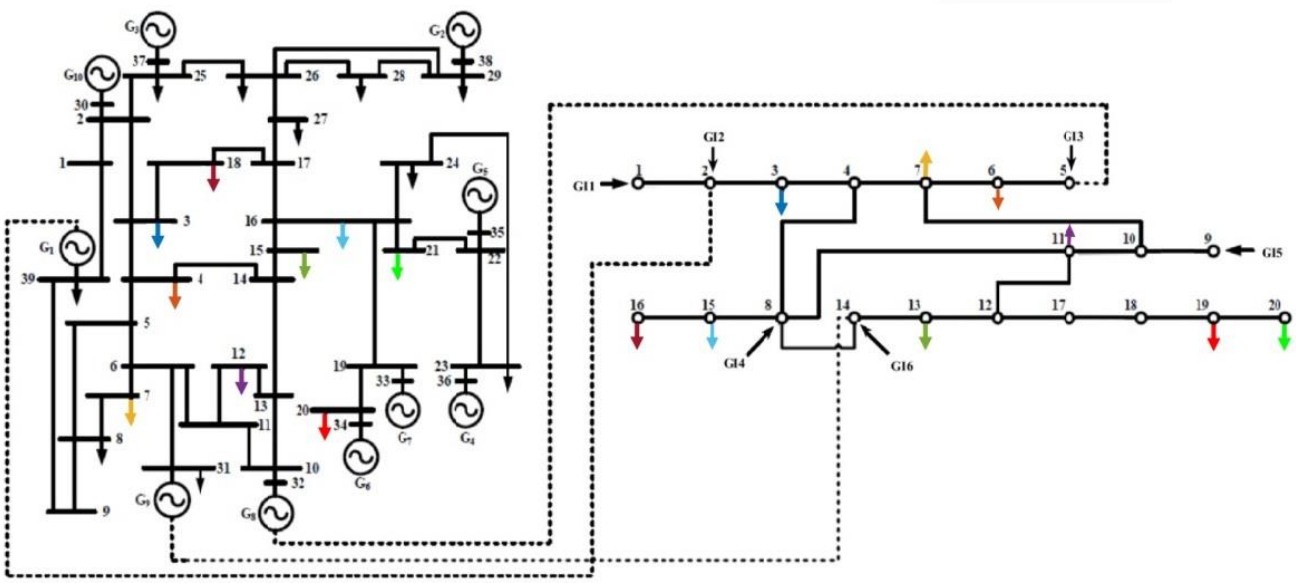

Fig.14: 39-bus electric power network-20-bus gas Belgian gas network.

The initial damage state in Fig. 15 is such that electrical generators G1 and G7 are completely disconnected from the network, whereas generators G10, G8, G9 and G5 are partially disconnected, that is important edges that connects them to the rest of the network are interrupted, e.g. the edge from node 13 to node 14 for G8. In the gas network, community nodes 19 and 20 are disconnected from the network, gas imports GI1, GI2 and GI3 are disconnected from most of the network and the redundant edge from node 8 to 11 sustains total disruption.

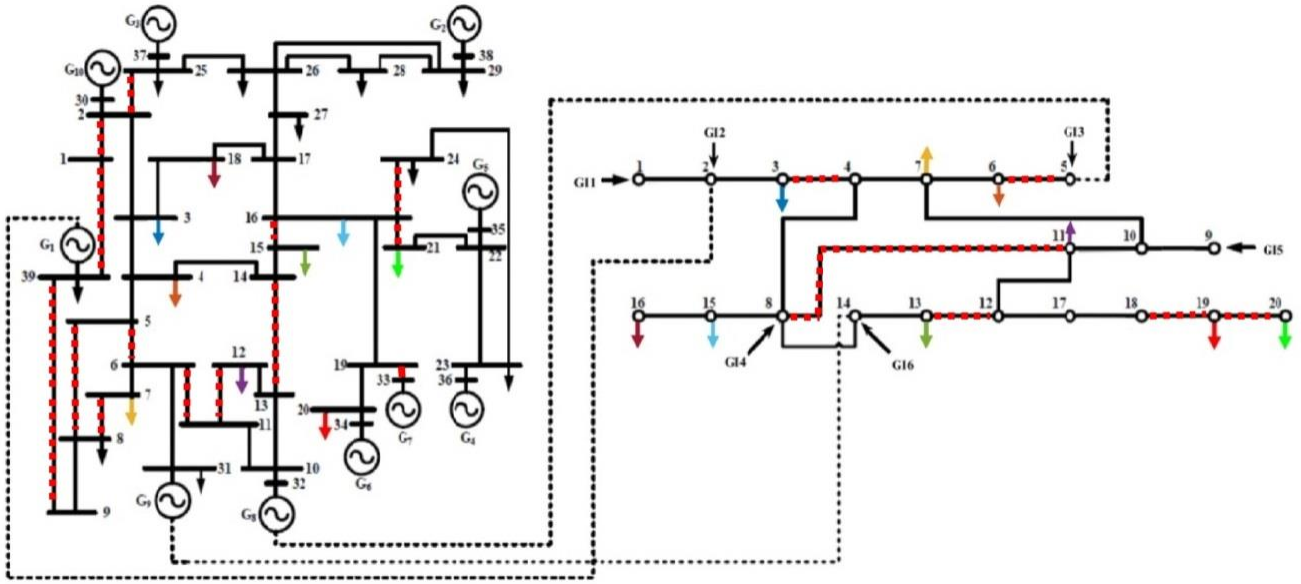

Fig.15: 39-bus electric power network-20-bus gas Belgian gas network initial damage state.

Fig. 16 shows the results of the recovery solution in the fourth and last week of the recovery process, as the restoration timeframe is still divided in $N_t = 4$ time intervals. The same conclusions obtained in section 3.3 for the smaller case study are observed also for the bigger case study. In particular, all the electrical generators are reconnected to the network, with the exception of generator G1, due to the electric load of node 39 in the immediate proximity.

The recovery of the gas network is coherent with the recovery of the electrical power network. In particular:

i) the recovery of the edge from node 3 to node 4 is neglected to sustain the gas load in node 3 and the gas supply to the generator G1;

ii) the recovery of the edge from node 5 to node 6 is neglected so that the gas import GI3 can be dedicated to sustain the production of generator G8;

iii) the redundant edge from node 8 to 11 is only mildly recovered as the import from GI4, GI5 and GI6 and the capacity of the surrounding edges are enough to sustain the load demands.

Finally, it is important to underline how more detailed models sustained by specific data to describe more realistically the Belgian infrastructure systems can guide the methodology towards a higher level solution to aid the system protection and restoration after a hazard occurrence.

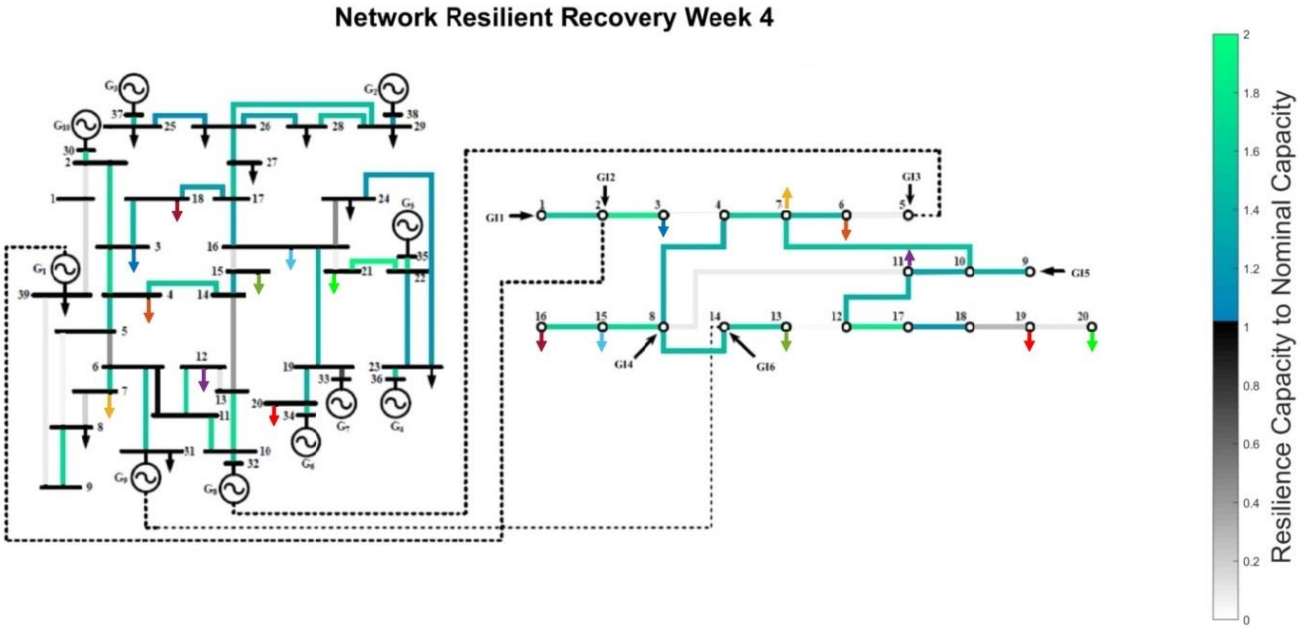

Fig.16: 39-bus electric power network-20-bus gas Belgian gas network recovery solution.

Chapter 5

Closure

5.1) Summary

This dissertation presents a methodology for the resilient recovery of interdependent infrastructure systems, from a disruptive hazard occurrence, guided by a multi-community decision making. A cooperative coevolution scheme is adopted to coordinate each module and tackle down the highly non-linear optimizations. A network-based definition of system resilience is proposed. The complete methodology embodies the key concepts of community resilience while relying on established infrastructure system theory items.

The model has a high degree of flexibility as each module is prone to be extended to the desired complexity and detail level, from community structure definition to system and network flow models.

An action level mapping strategy is proposed, by not restricting the community decision to a particular energetic strategy or predefined structure of specific network recovery actions. Moreover, a community decision making model based on network recovery performance and demand not served is also proposed.

An application to benchmark network case studies is carried on to critically asses the results. The capability of the network to explore different network recovery configurations is verified by running several independent recovery simulations from the same initial damage state and compare the best cases. Finally the recovery methodology is tested on a bigger benchmark case study to address the scalability of the model.

5.2) Conclusions

The main conclusions of the methodology can be summarized as follows:

- The results demonstrate the capability of the methodology to provide useful answers to the resilient recovery planning from a disruptive hazard scenario.
- The simulation model produces a coordinated solution between communities that succeeds in restoring the functionality of the infrastructure systems, as all electrical generators and gas imports are reconnected to the network, all communities' electric and gas loads are satisfied and the edges components are strengthened.
- The solution methodology is capable of considering different network recovery configurations from the same initial damage states. This unravels how additional constraints for specific applications can guide the solution to the desired outcome.
- The action levels are appropriate in the described recovery methodology, as they can be used effectively in the optimization programs as decision variables.
- The network modeling approach is appropriate in the context of infrastructure system resilience, as different objectives and constraints can be added based on the specific application.
- The methodology is flexible, as each part of the can be expanded with more detailed models and more in depth and specific analysis can be carried on.

The methodology is still a first stage approach and therefore not optimal for large or real system applications. Nevertheless, the coherency of the results and the cooperative coevolution approach capability to embed in single structure a multi-objective problem makes the methodology promising for future applications.

5.3) Future Work

The most immediate direction is to improve the methodology computational burden, so that it could be tested on real case studies.

Furthermore, in future works the model could be expanded to consider the recovery of transmission substations by introducing a physical flow model. An energy hub model [10,24] for communities, with which to describe more precisely community specific energetic strategies, can be thought to be coupled with multi-commodity network model. This integration can be exploited to investigate the impact of different system configurations, community energetic strategies and agents' decision making to the resilient recovery of the infrastructure system for the multi-community network.

Moreover, an efficient and optimized version of the methodology could be exploited to investigate the penetration of specific kind of energetic solutions to community resilience. A surrogate model for the system dynamics, through an artificial neural network approach could be a viable option in this case [31].

Bibliography

[1] Antenucci A, Sansavini G. Adequacy and security analysis of interdependent electric and gas networks. Proceedings of the Institution of Mechanical Engineers, Part O: Journal of Risk and Reliability 2018;232(2):121-39.

[2] Antenucci A, Sansavini G. Gas-Constrained Secure Reserve Allocation With Large Renewable Penetration. IEEE Transactions on Sustainable Energy 2018;9(2):685-94.

[3] Bazaraa MS, Jarvis JJ, Sherali HD. Linear programming and network flows. : John Wiley & Sons; 2011.

[4] Bruneau M, Chang SE, Eguchi RT, Lee GC, O'Rourke TD, Reinhorn AM, et al. A framework to quantitatively assess and enhance the seismic resilience of communities. Earthquake Spectra 2003;19(4):733-52.

[5] Chen L, Miller-Hooks E. Resilience: an indicator of recovery capability in intermodal freight transport. Transportation Science 2012;46(1):109-23.

[6] Coello CAC. Theoretical and numerical constraint-handling techniques used with evolutionary algorithms: a survey of the state of the art. Comput.Methods Appl.Mech.Eng. 2002;191(11-12):1245-87.

[7] Cox Jr, Louis Anthony Tony. Community resilience and decision theory challenges for catastrophic events. Risk analysis 2012;32(11):1919-34.

[8] Cutter SL, Barnes L, Berry M, Burton C, Evans E, Tate E, et al. A place-based model for understanding community resilience to natural disasters. Global Environ.Change 2008;18(4):598-606.

[9] Eusgeld I, Kröger W, Sansavini G, Schläpfer M, Zio E. The role of network theory and object-oriented modeling within a framework for the vulnerability analysis of critical infrastructures. Reliab.Eng.Syst.Saf. 2009;94(5):954-63.

[10] A modeling and optimization approach for multiple energy carrier power flow. Power Tech, 2005 IEEE Russia: IEEE; 2005.

[11] Geidl M, Andersson G. Optimal power flow of multiple energy carriers. IEEE Trans.Power Syst. 2007;22(1):145-55.

[12] Modeling integrated energy transportation networks for analysis of economic efficiency and network interdependencies. Proc. North American Power Symposium (NAPS); 2003.

[13] Gurobi Optimization Inc. Gurobi optimizer reference manual. 2014;.

[14] He X, Cha EJ. Modeling the damage and recovery of interdependent critical infrastructure systems from natural hazards. Reliab.Eng.Syst.Saf. 2018.

[15] Kröger W, Zio E. Vulnerable systems. : Springer Science & Business Media; 2011.

[16] Kröger W. Critical infrastructures at risk: A need for a new conceptual approach and extended analytical tools. Reliability Engineering & System Safety 2008;93:1781-7.

[17] Lavelle FM, Ritchie LA, Kwasinski A, Wolshon B. Critical assessment of existing methodologies for measuring or representing community resilience of social and physical systems. National Institute of Standards and Technology Government Contractor Report 2015.

[18] Bing Li. Assessment of Cascading Failure Risks and Development of Mitigation Strategies, PhD Thesis.ETH Zurich; 2018.

[19] YALMIP: A toolbox for modeling and optimization in MATLAB. Computer Aided Control Systems Design, 2004 IEEE International Symposium on: IEEE; 2004.

[20] Martin S, Ouelhadj D, Smet P, Berghe GV, ÖZcan E. Cooperative search for fair nurse rosters. Expert Syst.Appl. 2013;40(16):6674-83.

[21] Martínez-Crespo J, Usaola J, Fernández JL. Optimal security-constrained power scheduling by Benders decomposition. Electr.Power Syst.Res. 2007;77(7):739-53.

[22] Matarrita-Cascante D, Trejos B, Qin H, Joo D, Debner S. Conceptualizing community resilience: Revisiting conceptual distinctions. Community Development 2017;48(1):105-23.

[23] Nateghi R. Multi-dimensional infrastructure resilience modeling: an application to hurricane-prone electric power distribution systems. IEEE Access 2018;6:13478-89.

[24] Orehounig K, Mavromatidis G, Evins R, Dorer V, Carmeliet J. Towards an energy sustainable community: An energy system analysis for a village in Switzerland. Energy Build. 2014;84:277-86.

[25] A cooperative coevolutionary approach to function optimization. International Conference on Parallel Problem Solving from Nature: Springer; 1994.

[26] Praks P, Kopustinskas V, Masera M. Probabilistic modelling of security of supply in gas networks and evaluation of new infrastructure. Reliab.Eng.Syst.Saf. 2015;144:254-64.

[27] Quelhas A, Gil E, McCalley JD, Ryan SM. A multiperiod generalized network flow model of the US integrated energy system: Part I—Model description. IEEE Trans.Power Syst. 2007;22(2):829-36.

[28] Reilly AC, Tonn GL, Zhai C, Guikema SD. Hurricanes and Power System Reliability-The Effects of Individual Decisions and System-Level Hardening. Proc IEEE 2017;105(7):1429-42.

[29] Renschler CS, Frazier AE, Arendt LA, Cimellaro GP, Reinhorn AM, Bruneau M. A framework for defining and measuring resilience at the community scale: The PEOPLES resilience framework. : MCEER Buffalo; 2010.

[30] Reza F, Miller-Hooks Elise. A Mathematical Framework for Quantifying and Optimizing Protective Actions for Civil Infrastructure Systems. Computer-Aided Civil and Infrastructure Engineering 2014 09/01; 2018/06;29(8):572-89.

[31] Rocchetta R, Zio E, Patelli E. A power-flow emulator approach for resilience assessment of repairable power grids subject to weather-induced failures and data deficiency. Appl.Energy 2018;210:339-50.

[32] Santoso T, Ahmed S, Goetschalckx M, Shapiro A. A stochastic programming approach for supply chain network design under uncertainty. Eur.J.Oper.Res. 2005;167(1):96-115.

[33] Shah AA, Ye J, Abid M, Khan J, Amir SM. Flood hazards: Household vulnerability and resilience in disaster-prone districts of Khyber Pakhtunkhwa province, Pakistan. Nat.Hazards 2018:1-19.

[34] Storn R. Differrential evolution-a simple and efficient adaptive scheme for global optimization over continuous spaces. Technical Report, International Computer Science Institute 1995;11.

[35] Su H, Zhang J, Zio E, Yang N, Li X, Zhang Z. An integrated systemic method for supply reliability assessment of natural gas pipeline networks. Appl.Energy 2018;209:489-501.

[36] Thorén H, Olsson L. Is resilience a normative concept? Resilience 2018;6(2):112-28.

[37] Tonn GL, Guikema SD. An Agent-Based Model of Evolving Community Flood Risk. Risk Analysis 2018;38(6):1258-78.

[38] Wang C, Wei W, Wang J, Liu F, Qiu F, Correa-Posada CM, et al. Robust Defense Strategy for Gas–Electric Systems Against Malicious Attacks. IEEE Trans.Power Syst. 2017;32(4):2953-65.

[39] Zhang X, Mahadevan S, Sankararaman S, Goebel K. Resilience-based network design under uncertainty. Reliab.Eng.Syst.Saf. 2018;169:364-79.